Editor in Chief Dr. Kouroush Jenab

International Journal of Engineering (IJE)

Book: 2008 Volume 2, Issue 3

Publishing Date: 30-06-2008

Proceedings

ISSN (Online): 1985-2312

IJE Journal is a part of CSC Publishers

http://www.cscjournals.org

Published in Malaysia

Typesetting: Camera-ready by author, data conversation by CSC Publishing Services – CSC Journals, Malaysia

CSC Publishers

Table of Contents

Volume 2, Issue 3, June 2008.

Analysis and Design Hilbert Curve Fractal Antenna Feed with Co-planar Waveguide for multi-band wireless communications

Niruth Prombutr egnpb@mahidol.ac.th
Faculty of Engineering/Electrical engineering department
Mahidol University
Nakornpathom,73170, Thailand

Prayoot Akkaraaektharin prayoot@kmutnb.ac.th
Faculty of Engineering/Electrical engineering department
King Mongkut's University of Technology North Bangkok
Bangkok, 10800,Thailand

Abstract

There are many techniques to improve the characteristic of antennas. In this work we use ideas of the fractal. The purpose of this project is to design and analyze Hilbert curve fractal antennas to get the empirical and electrical model. We use the Zealand program for simulating antennas. The antennas receive and transmit in many frequency resonances. We design a small Hilbert curve fractal antenna. We analyze this antenna by using the concept of the CPW transmission line and the mathematical definition of fractal to yield the models for Hilbert curve fractal antenna. From these models we can predict the multi resonance frequency. In the experiment we found that the least percent of difference for electromagnetics formular model with the experiment (0.4%) is lower than the least of the difference for empirical model (4.43%) because the electromagnetics model used the transmission line model while the empirical model used the numerical method. These models will be helpful for design and making Hilbert curve fractal antenna.

Keywords: Fractal antenna, Multi-band, Hilbert curve, Electromagnetics model, Coplanar waveguid feed.

1. INTRODUCTION

The term fractal was coined by the French mathematician B.B. Mandelbrot during 1970's after his pioneering research on several naturally occurring irregular and fragmented geometries not contained within the realms of conventional Euclidian geometry [1].The use of fractal geometries has significantly impacted many areas of science and engineering; one of which is antennas. Antennas using some of these geometries for various telecommunications applications are already available commercially. The use of fractal geometries has been shown to improve several antenna features to varying extents. Yet a direct corroboration between antenna characteristics and geometrical properties of underlying fractals has been missing. This research work is intended as a first step to fill this gap. In terms of antenna performance, fractal shaped geometries are believed to result in multi-band characteristics and reduction of antenna size. A quantitative link between multi-band characteristics of the antenna and a mathematically expressible feature of the fractal geometry is needed for design optimization. To explore this, we

design the Hilbert curves fractal antenna that use the coplanar wave guide feed. This has been explored numerically and validated experimentally. One of the advantages of using fractal geometries in small antennas is the order associated with these geometries in contrast to an arbitrary meandering of random line segments (which may also result in small antennas). However this fact has not been used in antenna design thus far. In this work, approximate expressions for designing antennas with these geometries have been derived incorporating their fractal nature. To conclude, the research work reported here is a numerical and experimental study in identifying features of fractal shaped antennas that could impart increased flexibility in the design of newer generation wireless systems.
Several antenna configurations based on fractal geometries have been reported in recent years [2] – [4]. These are low profile antennas with moderate gain and can be made operative at multiple frequency bands and hence are multi-functional. In this work the multi-band (multifunctional) aspect of antenna designs are explored further with special emphasis on identifying fractal properties that impact antenna multi-band characteristics. Antennas with reduced size have been obtained using Hilbert curve fractal geometry. Further more, design equations for these antennas are obtained in terms of its geometrical parameters such as fractal dimension. One of the fundamental advantages of using a fractal geometry in antennas is reducing the size of a resonant antenna. This is very evident in dipole and monopole antennas using fractal Koch curves [5], and some of their modifications in the form of closed loops, and Minkowski curves [6]. The ability of these geometries to pack longer curves within relatively smaller area is the salient aspect in their use in antennas. Being a plane filling geometry, Hilbert curves can enclose longer curves for a given area than Koch curves [7].

2. Hilbert Curve Fractal antenna

2.1 Axioms L system for Hilbert Curve

The first few iterations of Hilbert curves are shown in Fig. 1. It may be noticed that each successive stage consists of four copies of the previous, connected with additional line segments. This geometry is a space-Filling curve, since with a larger iteration, one may think of it as trying to fill the area it occupies. Additionally the geometry also has the following properties: self-Avoidance (as the line segments do not intersect each other), Simplicity (since the curve can be drawn with a single stroke of a pen) and self-Similarity (which will be explored later). Because of these properties, these curves are often called an FASS curves [8].

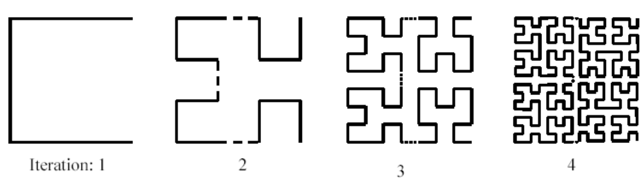

FIGURE 1: First four iterations of Hilbert curve geometry.

The segments used to connect copies of the previous iteration are shown in dashed lines. The generation algorithm of this geometry is commonly expressed in terms of L-systems. In this representation, a string of symbols with the following notations are used, leave two blank lines between successive sections as here.

(1)

(2)

where is moving forward a step, + is turn left by , - is turn right by . A recursive approach may be used to generate higher iterations (is integer = 0, 1, 2, …) of the geometry from these

(3)

(4)

2.2 Antenna Configurations Using Hilbert Curves

It would be interesting to study the properties of a new antenna with reference to various existing, and more familiar antennas. In this context, a schematic of the thought process leading to the Hilbert curve antenna. The half-wave meander line antenna is resonant when the arms are approximately quarter wavelength long. The biconical antenna is a broadband variant for the common dipole [9]. This antenna can even be simulated with wires along its periphery. Puente et al [2] have used a bowtie as the base model for explaining the properties of the Sierpinski gasket fractal antenna with multi-band radiation characteristics.

A conventional coplanar waveguide (CPW) on a dielectric substrate consists of a center strip conductor with semi-infinite ground planes on either side as shown in Fig 2. This type of antenna offers several advantages over microstrip line. It simplifies fabrication, facilitates easy shunt as well as series surface mounting of active and passive devices, eliminates the need for via holes and reduces radiation loss. In addition a ground plane exists between two adjacent lines; hence cross talk effects between them are very week. As a result, CPW circuits can be made denser than microstrip circuits [9].

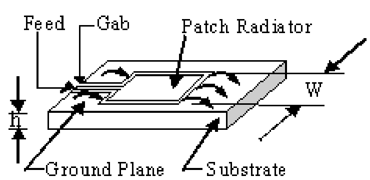

FIGURE 2: CPW antenna

CPW antennas are designed by using the IE3D program. This program has high efficiency, accuracy and low cost simulation tools. The proposed antenna is excited by a CPW line of 50 Ω and is fabricated on a FR4 substrate with a thickness (h) of 1.6 mm and relative permittivity ( ) of 4.4. The two ground planes are placed symmetrically on each side of the CPW line. Design the fundamental resonance frequency at 1.8 GHz for the first stage of Hilbert curve antenna shown in Fig 3.

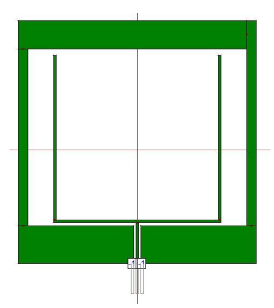

a)

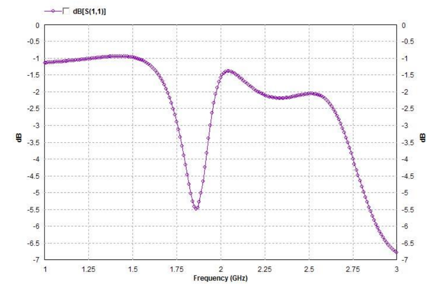

b)

FIGURE 3 : a) First stage of Hilbert curve geometry. b) the return loss of this stage

We design the next stage of this Hilbert curve antenna(stage 2, 3,and 4) and study the return loss response of each stage that shown in the Fig. 4,5 and 6 respectively. We found that the number of resonance frequency increase that satisfy the concept of fractal antenna.

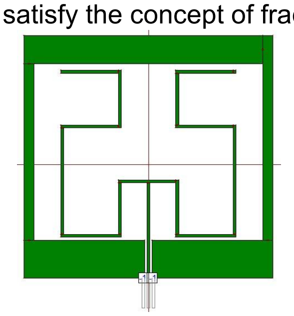

a)

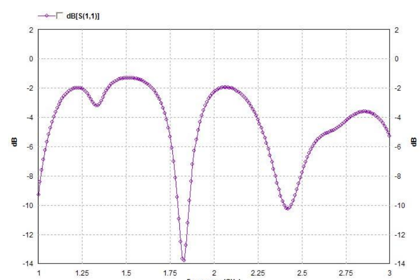

b)

FIGURE: 4 a) second stage of Hilbert curve geometry. b) the return loss of this stage

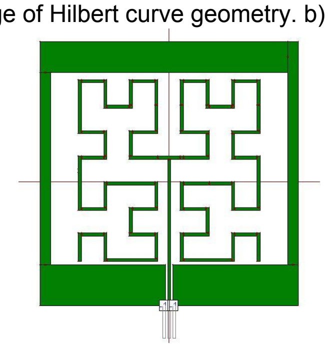

a)

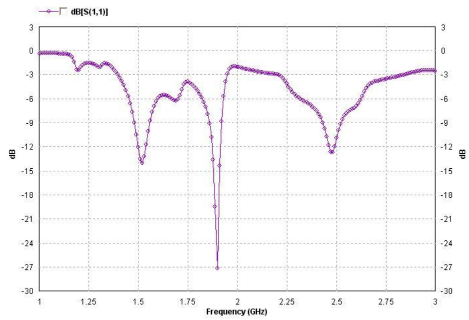

b)

FIGURE: 5 a) third stage of Hilbert curve geometry. b) the return loss of this stage

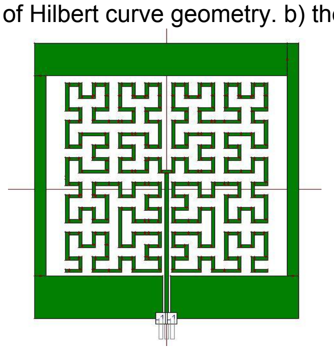

a)

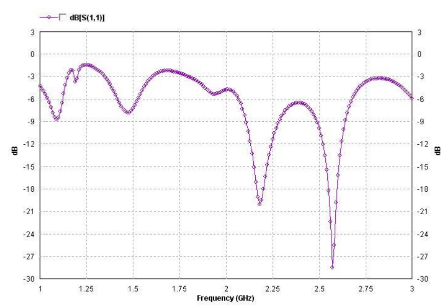

b)

FIGURE: 6 a) fourth stage of Hilbert curve geometry. b) the return loss of this stage

3. Result

We made this Hilbert Curve antenna by using the fabrication on the FR-4 substrate that shown in Fig. 7. The proposed antennas have been tested using a calibrated vector network analyzer. Measured result of the return loss(S_{11}) compared with the simulation is shown in Fig. 8.

FIGURE: 7 The photograph of proposed Hilbert curve antenna at stage 4

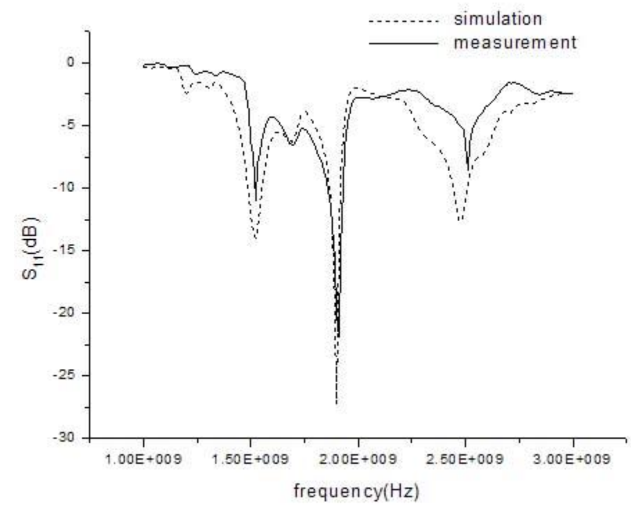

FIGURE: 8 Measured result of S11 compared with the simulation

The far-field radiation patterns of the proposed antenna have been measured by connecting transmitting antenna to the frequency sweep generator and connecting the receiving antenna to the spectrum analyzer. Measured results of the patterns had been plotted in Fig 9.

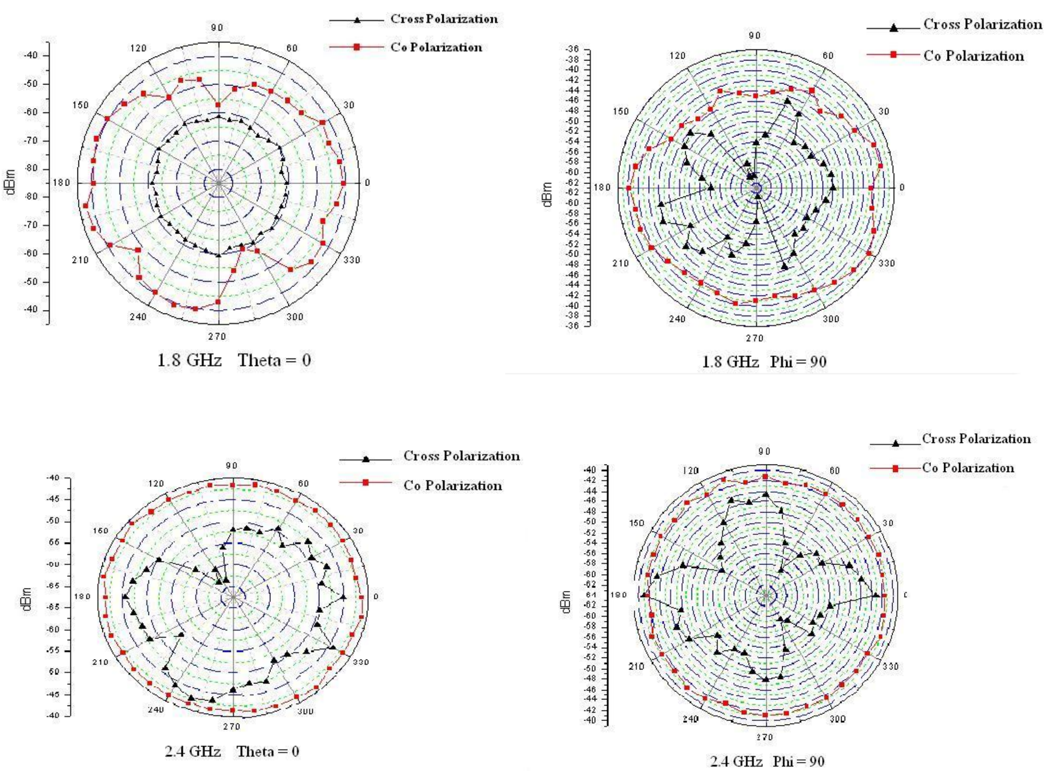

FIGURE: 9 Measured result of the patterns for the proposed CPW antennas

4 Analyze and Design formula

4.1 EMPIRICAL MODEL

It is now possible to obtain approximate design equations for this type of antenna. The approach for the design formulation is based on that followed for resonant meander line antennas [10].

The resonant frequencies are obtained through the above formulation by use the numerical method. We can find the empirical model equation by using the basic concept of antenna that state the resonance frequency vary inversely with the size of the antenna as shown in the Fig. 10

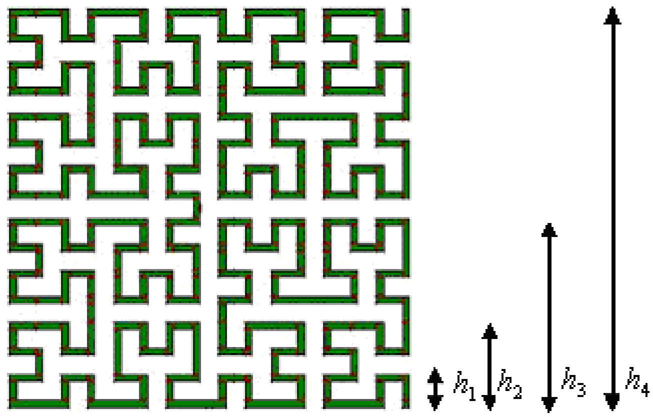

FIGURE: 10 Dimension of Hilbert Curve Fractal Antenna iteration 4 at the first fourth resonance frequency.

From this design HCFA, the dimensions of antenna are h_4=88 mm, h_3=44 mm, h_2=22 mm, and h_1=7.266 mm. This antenna wills resonance at 0.84 GHz, 1.52 GHz 1.9GHz and 2.48 GHz that satisfy the size of antenna as shown in the table 1

n(band)	f_n(GHz)	f_{n+1}/f_n (δ)	h_n/λ_n
1	0.840	1.803	0.2464
2	1.520	1.254	0.2229
3	1.900	1.302	0.14
4	2.480	1.381	-

TABLE:1 The dimension of Hilbertcurve antenna at difference Resonance frequency

From the data we found that the ratio of the next stage resonance frequency to this stage will converge to some number (1.38) that we call log period and the ratio of the height to the resonance wavelength seem to be constant about 0.21(average of 0.2464, 0.2229, 0.14) that we use this coefficient in the proposed model. Finally the data has been analyzed resulting in an empirical model formula at resonance stage n

(5)

where f_n = the resonance frequency at stage n

c= speed of electromagnetic wave= m/s
h = the highest dimension size of antenna
n = integer number at stage n (1,2,3,.,.)
δ = log period = 1.38

The resonance frequency from above model and simulation are compared with simulation. A table of comparison is given below (Table 2). From the table, the percent of difference will be smaller at the higher resonance frequency. These antennas are fabricated on a FR4. These results show a reasonable match between the simulation and empirical model, and hence it is concluded that the above formulation may be used as an empirical design equation for antennas of this type.

4.2 Electromagnetics Model

It is now possible to obtain approximate design equations for this type of antenna. The approach for the design formulation is based on that followed for resonant meander line antennas [10]. In this approach, the inductances of the turns of the meander line are calculated, considering them as short circuited parallel-two-wire lines. The self inductance of an imaginary straight line connecting all these turns is then added to this to get the total inductance. This is then compared with the inductance of a regular half wavelength meander line. Since meander line antennas with approximately half wavelength are resonant (their capacitive and inductive reactances cancel each other)[11], and assuming that the input capacitive reactance for a meander line antenna remains unchanged by reducing its apparent length by introducing turns, the resonant condition for this antenna is derived. The approach reported in [12] for the meander line meander line antenna can readily be extended for the Hilbert curve antenna (HCA). The definition of self inductance of a straight line for meander line antenna is replaced here with the total inductance of the line segments otherwise unaccounted (not forming short-circuited parallel wire sections). Another important assumption is that the capacitances of the meander line configurations remain the same in all cases. For an HCA (Fig. 10) with outer dimension of and order of fractal iteration n, the length of each line segment d is given by

(6)

The number of short circuit terminations for parallel wire section be founded that

(7)

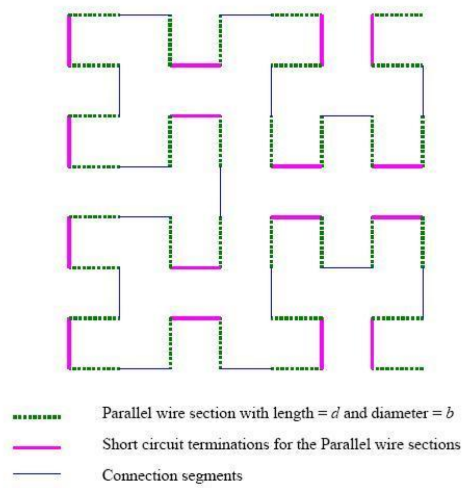

FIGURE: 11 Composition of a HCA with iteration order 3. The short-circuited parallel wire sections and connection wire sections are shown separately.

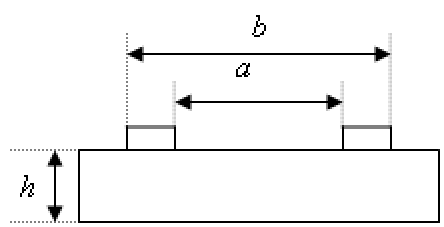

FIGURE:12 Cross section of the Coplanar Waveguide Hilbert Curve Fractal Antenna.

The segments not forming the parallel wire sections amount to a total length is

(8)

The approach we introduce to derive the condition for the resonant properties of Hilbert curve antennas printed on a dielectric substrate, is to consider sections of the strip as terminated parallel strip transmission lines. The characteristic impedance of two parallel strips of negligible thickness (t) printed on a dielectric of height (h), and dielectric constant , as shown in Fig.11 in terms of complete elliptic integral of the first kind (K) is given by [12]:

(9)

where the effective dielectric constant is

and the pure inductance is

(10)

The self inductance due to a straight line of length s as

(11)

Substituting (9) in (10) and using (11), the total inductance is therefore

(12)

It should however be noted that regular meander line antennas resonate when the arm length is a multiple of quarter wavelength. Thus, by changing the resonant length related terms on the RHS of equation, we can obtain all the resonant frequencies of the multi-band HCA. Therefore the first few resonant frequencies of the HCA can be obtained from the formula model:

(13)

where k is an odd integer (1,3,5,…) and

=propagation characteristics of the transmission line.

The resonant frequencies were obtained through the above formulation by use the numerical method to iterate the frequencies that make the LHS equal RHS. The resonance frequency from above model and simulation were compared with experiments. A table of comparison is given below (Table 2). From the table 2, these models will be more accurate at the higher frequency. These antennas are fabricated on a FR4. These results show a reasonable match between the two, and hence it is concluded that the above formulation may be used as an empirical design equation for antennas of this type.

	Resonant Frequency(GHz)

	f_{r1}	f_{r2}	f_{r3}
Simulation	1.52	1.90	2.48
Empirical Model (Percent of Difference)	1.36 (10.52%)	1.87 (1.57%)	2.59 (4.43%)
Electromagnetics Model (Percent of Difference)	1.45 (4.6%)	1.96 (3.15%)	2.47 (0.4%)

TABLE: 2 Comparison of formulation with experimental simulation results for Hilbert curve antennas printed

5. Conclusion

In this work the development of antennas using Hilbert curve fractal geometry is presented. Some of the numerical results are validated through experiments and we found that the least percent of difference for this empirical model is 4.43%. The advantage of numerical method for this work is easy because when we consider empirical model, this model gives the higher percentage of difference than the electromagnetics model that gives the least percentage of difference for this model(0.4 %). These models will be helpful for design Hilbert curve fractal antennas. The numerical results presented in this research indicate that further reduction in resonant frequency is possible for Hilbert curves. A patch configuration is also explored. However, the antenna characteristics in this configuration are found to be dictated by the outer dimensions.

6. References

1. B.B. Madelbrot, *The Fractal Geometry of Nature*, New York: W.H. Freeman, 1983
2. C. Puente, J. Romeu, R. Bartoleme, and R. Pous, *“Fractal multiband antenna based on Sierpinski gasket,”* Electron. Lett., vol. 32, pp. 1-2, 1996.
3. C. Puente-Baliarda, J. Romeu, R. Pous, J. Ramis, and A. Hijazo, *“Small but long Koch fractal monopole,”* Electron. Lett., vol. 34, pp. 9-10, 1998.
4. N. Cohen, *“Fractal antenna applications in wireless telecommunications,”* in Professional Program Proc. of Electronics Industries Forum of New England, 1997,IEEE, pp. 43-49, 1997
5. C.P. Baliarda, J. Romeu, and A. Cardama, *“The Koch monopole: A small fractal antenna,”* IEEE Trans. Ant. Propagat., vol. 48 pp. 1773-1781, 2000.
6. J.P. Glanvittorio and Y. Rahmaat-Samii, *“Fractal element antennas: A compilations of configurations with novel characteristics,”* IEEE AP-S Inter. Symp. 2000, pp.1688-1691, 2000.
7. V K.J. Vinoy, K.A. Jose, V.K. Varadan, and V.V. Varadan, *“Hilbert curve fractal antenna: a small resonant antenna for VHF/UHF applications,”* Microwave & Optical Technology Letters, vol. 29, pp. 215-219, 2001.
8. H.-O. Peitgen, J.M. Henriques, L.F. Penedo (Eds*.),”Fractals in the Fundamental and Applied Sciences”*, Amsterdam: North Holland, 1991
9. Niruth Prombutr, Jarinthip Pakeesirikul, Theerayut Theatmongkol, Samuttachai Suangool, *“Dual-band Coplanar Waveguide Antenna Design by using U-Slot with diagonal edge,”* The 21st International Technical Conference on Circuits/Systems, Computers and Communications, vol III, pp 117-120, Chaingmai, 2006.
10. T. Endo, Y. Sunahara, S. Satoh, and T. Katagi, *“Resonant frequency and radiation efficiency of meander line antennas,”* Electronics & Commun. in Japan, Pt. 2, vol.83, pp. 52-58, 2000.
11. C.A. Balanis, *Antenna Theory: Analysis and Design*, New York: John Wiley (2nd Ed.), 1997.
12. B.C. Wadell, *Transmission Line Design Handbook*, Dedham Artech House, 1991.

Enhancing the 'Willingness' on the OLSR Protocol to Optimize the Usage of Power Battery Power Sources Left

Saaidal Razalli Azzuhri saaidal@um.edu.my
Electrical Engineering Department, Faculty of Engineering
University of Malaya
Kuala Lumpur, 50603 Federal Territory, Malaysia

Suhazlan Suhaimi suhazlan@ftmk.upsi.edu.my
Faculty of Information & Communication Technology
Sultan Idris Education University
Tanjong Malim, 35900 Perak, Malaysia

K. Daniel Wong dwong@must.edu.my
Department of Information Technology
Malaysia University of Science & Technology
Petaling Jaya, 47301 Selangor, Malaysia

Abstract

Mobile ad-hoc networks are infrastructure-free and highly dynamics wireless networks. There are many routing protocols for Mobile Ad Hoc Networks (MANET). One of the popular routing protocols is Optimized Link State Routing (OLSR). OLSR was developed to work independently from higher-layer protocols and it creates an underlying architecture for communication without the help of traditional fixed-position routers. In addition, OLSR attempts to maintain the communication routes for the mobile nodes that have limited transmission range. This paper discusses the OLSR implementation in terms of battery power status and its advantages particularly pertaining to the relationship between the power status function with the OLSR by modify some of the OLSR source code. The study also focuses on maximizing the use of the battery power sources. The results from the experiment show that the usage of the battery power sources left was maximally used when the “Willingness” for the nodes was indeed increased. We will conclude that the experiments have been successfully done and the results demonstrate the improvement for the OLSR nodes to maximize the battery power sources usage on the MANET by enhancing the “Willingness” on the OLSR protocol.
+

Keywords: Multipoint-relay, ad-hoc, cross platform, OLSR, MANET

1. INTRODUCTION

A Mobile Ad Hoc Networks (MANET) is an autonomous system of mobile nodes. It consists of mobile platforms for example a router with multiple hosts and wireless communications devices. Herein simply referred to as 'nodes' which are free to move about arbitrarily. It also may operate in isolation or may have gateways to and interface with fixed network. There are many important research questions in MANET. However, power efficiency is one of the most important issues. It is important to realize that issues such as QoS support, TCP performance, speed of routing repair process and others are secondary if nodes have a high probability of running out of energy resources. Energy awareness in wireless ad hoc networks actually spans across several communication layers. Advances in battery technology are very slow compared to the results achieved in integrated circuit technology particularly in comparison to the rate of growth in communication speeds. Therefore, saving transmission power represents one of the most significant methods for long term wireless system performance.

In OLSR, the power energy resource is a very important factor in deciding whether the node can forward a packet or not. It is because only nodes where the “Willingness” is bigger than 7 can be used to forward packets. The higher the willingness of the node the higher the chance it will be selected as an MPR (we will explain the terms “willingness” and MPR later). The nodes willingness is based on the power resources it has from AC power sources or from the battery. There is no power problem when the nodes are using the power from the AC power sources as the nodes will get power consistently. However, problems may occur when the nodes use the power from the battery in which the power is limited. On the other hand, the MANET nodes are usually used in scenarios without any infrastructure, and therefore without AC power sources [1]. Thus, it is important to optimize the usage of the limited resources from the battery.

2. BACKGROUND THEORY

2.1. OPTIMIZED LINK STATE ROUTING (OLSR)

The Optimized Link State Routing Protocol (OLSR) is a protocol that was developed for mobile ad hoc network (MANET). It is a variation of traditional link state routing, modified for improved operation in ad hoc networks. It is a table driven and proactive routing protocol where the nodes exchange their topology information with other nodes regularly. The routes in the proactive protocols are always immediately available when needed [2]. OLSR is designed to work in a completely distributed manner and does not depend on any central entity. The protocol does not require reliable transmission of control messages. Each node sends control messages periodically and sustains a reasonable loss of some such messages. Such losses occur frequently in radio networks due to collisions or other transmission problems.

The key feature of this protocol is multipoint relays (MPRs). Topological changes cause floods of the topological information to all available nodes in the network. Therefore, the multipoint relays (MPRs) are used to reduce the overhead of network floods and size of link state updates. Every node selects a set of its neighbour nodes as multipoint relays (MPRs). Only MPRs nodes are responsible for forwarding control traffic. MPRs nodes only declare link-state information when the requirements for OLSR provide the shortest path information message [3]. The neighbours, whom the node selects as MPR, announce this information periodically in their ‘Control Message’. In route calculation, the MPRs are used to form the route from a given node to any destination in the network. It is also be used to facilitate efficient flooding of Control Message in the network. OLSR uses two kinds of Control Messages; Hello Messages and Topology Control messages.

2.1.1.HELLO MESSAGE

Each node should detect the neighbour nodes with which it has a direct and symmetric link. The uncertainties over radio propagation may make some links asymmetric. Consequently, all links MUST be checked in both directions in order to be considered valid. To accomplish this, each node broadcasts HELLO messages, containing information about neighbours and their link status. The link status may either be "symmetric", heard" (asymmetric) or "MPR". "Symmetric" indicates that the link has been verified to be bi-directional, for example, it is possible to transmit data in both directions. "Heard" indicates that the node can hear HELLO messages from a neighbour, but it is not confirmed that this neighbour is also able to receive messages from the node. "MPR" indicates that a node is selected by the sender as a MPR. A status of MPR further implies that the link is symmetric. These control messages are broadcast to all one-hop neighbours, but are *not relayed* to further nodes. A HELLO-message contains [4]:

- A list of addresses of neighbours, to which there exists a symmetric link.

- A list of addresses of neighbours, which have been "heard".
- A list of neighbours, which have been selected as MPRs.

The list of neighbours in a HELLO message can be partial (for example, due to message size limitations, imposed by the network), the rule being that all neighbour nodes are cited at least once within a predetermined refreshing period (HELLO_INTERVAL).

2.1.2.TOPOLOGY CONTROL (TC)

In order to build the topology information base needed, each node, which has been selected as MPR, broadcasts Topology Control (TC) messages. TC messages are flooded to all nodes in the network and take advantage of MPRs. MPRs enable a better scalability in the distribution of topology information. A TC message is sent by a node in the network to declare its MPR Selector set. For example, the TC message contains the list of neighbours which have selected the sender node as a MPR. The information diffused in the network by these TC messages will help each node to calculate its routing table. A node which has an empty MPR selector set, such as nobody has selected it as a MPR, MUST NOT generate any TC message.

2.1.3.CONTROL TRAFFIC

All OLSR control traffic is transmitted over UDP on port 698. The Internet Assigned Numbers Authority (IANA) assigns this port to OLSR. The RFC states that this traffic is to be broadcasted when using IPv4 however, no broadcast address is specified. It is implicitly understood that one must use a multicast address when using IPv6 as IPv6 does not have broadcast addresses, even though it is not specified in the RFC [5]. FIGURES 2.1 and 2.2 shows the paths information is passed when being spread, first using regular flooding, then using MPR flooding. The number of retransmissions in a MPR scenario highly depends on the network topology and the MPR calculation algorithm. However, using the same topology as in FIGURE 2.3, a possible MPR calculation could lead to the yellow nodes in FIGURE 2.4 being chosen as MPRs by the center node. As one can see, if the center node is to flood a message throughout the network, four retransmissions are done using MPR as opposed to 24 using traditional flooding.

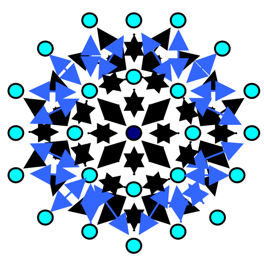

FIGURE 2. 1: Flooding a packet in a wireless multihop network. The arrows show all transmission (T. Andreas, 2004).

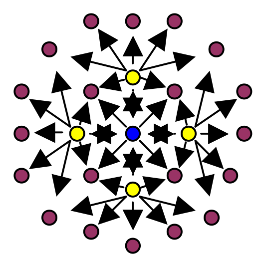

FIGURE 2. 2: Flooding a packet in a wireless multihop network from a centre node using MPRs (Yellow). The arrows show all transmission (T. Andreas, 2004)

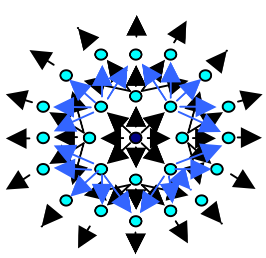

FIGURE 2. 3: Flooding a packet in a wireless multihop network. The arrows show the way information is passed but not to all transmission (T. Andreas, 2004).

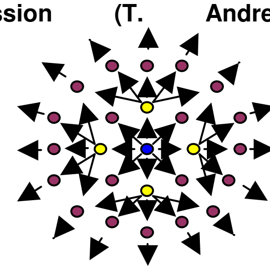

FIGURE 2. 4: Flooding a packet in a wireless multihop network from a centre node using MPRs (Yellow). The arrows show the way information is passed but not to all transmission (T. Andreas, 2004).

2.1.4.ROUTING

LINK SENSING

Link Sensing is accomplished through periodic emission of HELLO messages over the interfaces through which connectivity is checked. A separate HELLO message is generated for each interface and emitted in correspondence with the provisions. Resulting from Link Sensing is a local link set which describing links between "local interfaces" and "remote interfaces" for example the interfaces on neighbour nodes. If sufficient information is provided by the link-layer, this may be utilized to populate the local link set instead of HELLO message exchange. Link sensing populates the local link information base. Link sensing is exclusively concerned with OLSR interface addresses and the ability to exchange packets between such OLSR interfaces. The mechanism for link sensing is the periodic exchange of HELLO messages.

The Link Set is populated with information on links to neighbour nodes. The process of populating this set is denoted "link sensing" and is performed using HELLO message exchange, updating a local link information base in each node. Each node should detect the links between itself and neighbour nodes. Uncertainties over radio propagation may make some links unidirectional. Consequently, all links MUST be checked in both directions in order to be considered valid. A "link" is described by a pair of interfaces: a local and a remote interface. For the purpose of link sensing, each neighbour node (more specifically, the link to each neighbour) has an associated status of either "symmetric" or "asymmetric". "Symmetric" indicates that the link to that neighbour node has been verified to be bi-directional, for example, it is possible to transmit data in both directions. "Asymmetric" indicates that HELLO messages from the node have been heard (for example, communication from the neighbour node is possible), however it is not confirmed that this node is also able to receive messages (for example, communication to the neighbour node is not confirmed). The information, acquired through and used by the link sensing, is accumulated in the link set. (A. Laoutti, P. Muhlethaler, A. Najid and E. Plakoo, 2002). The process will illustrate as a FIGURE 2.5.

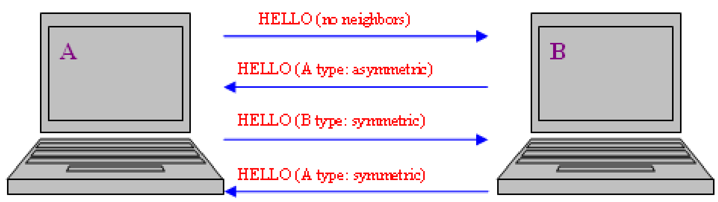

FIGURE 2.5: A typical neighbour discovery session using HELLO message

MULTIPOINT RELAYS

The Multipoint Relays (MPR) is the key idea behind the OLSR protocol in order to reduce the information exchange overhead. In OLSR only the MPRs can forward the data throughout the network. Each node must have the information about the symmetric one hop and two hop neighbours in order to calculate the optimal MPR set. The two hop neighbours are found from the Hello message because each Hello message contains all the nodes' neighbours [7]. FIGURE 2.6 shows the multipoint relays (MPRs) selection between its neighbours. For instance node A select m1, m2 and m3 nodes. When node A floods a message, only node m1, node m2 and nod m3 re-transmit it, after that the MPRs of node m1, node m2 and node m3 retransmit and so on. There are 2 rules to select a node for MPR:

- First, any 2-hop neighbour must be covered by at least one multipoint relay.
- Second, try to minimize the number of multipoint relays.

Then a node forwards a flooding packet according to several rules. The multipoint relays idea is to reduce the redundant retransmissions in the same region by minimizing the overhead of flooding message in the network. Each node in the network selects a set of nodes in its symmetric 1-hop neighbourhood, which may retransmit its messages. This set of selected neighbour nodes is called the "Multipoint Relay" (MPR) set of that node. The neighbours of node N which are *NOT* in its MPR set, receive and process broadcast messages but do not retransmit broadcast messages received from node N.

Each node selects its MPR set from among its 1-hop symmetric neighbours. This set is selected such that it covers (in terms of radio range) all symmetric strict 2-hop nodes. The MPR set of N, denoted as MPR (N), is then an arbitrary subset of the symmetric 1-hop neighbourhood of N, which satisfies the following condition: every node in the symmetric strict 2-hop neighbourhood of N must have a symmetric link towards MPR (N) (FIGURE 2.7). The smaller a MPR set, the less control traffic overhead results from the routing protocol gives an analysis and example of MPR selection algorithms.

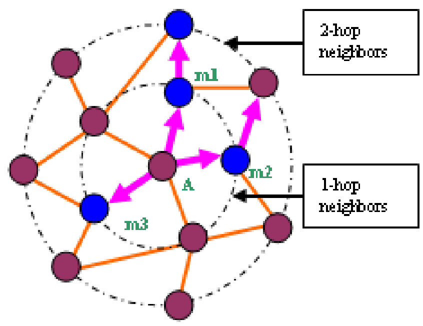

FIGURE 2.6: The Selection of MPRs among its neighbours.

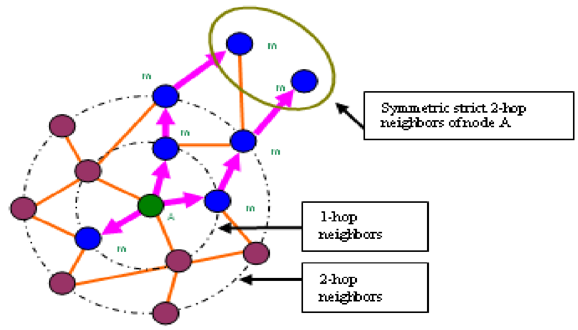

FIGURE 2.6: Symmetric strict 2-hop neighbours of node A

Each node maintains information about the set of neighbours that have selected it as MPR. This set is called the "Multipoint Relay Selector set" (MPR selector set) of a node. A node obtains this information from periodic HELLO messages received from the neighbours. A broadcast message, intended to be diffused in the whole network, coming from any of the MPR selectors of node N is assumed to be retransmitted by node N, if N has not received it yet. This set can change many time (for example, when a node selects another MPR-set) and is indicated by the selector nodes in their HELLO messages. Another rule that apply here is re-emitting rule that is shown in FIGURE 2.8. In FIGURE 2.8, if node m5 receives from node m2 first, it will re-transmit but, if the node m5 receives from node m1, it will not re-transmit. It means that no node will be missed when OLSR is used.

SHORTEST PATH WITH MPR LINKS

The MPR links offer a sparse partial topology containing the shortest paths. Any 2-hop neighbour of n node of a source of A node must have selected by some neighbours of A node as a MPR since an A node is a 2-hop neighbour of n node. Indeed, any node at distance m6 node from A node must have selected as MPR. Thus, it used MPR links backward to route from A node to m6 node.

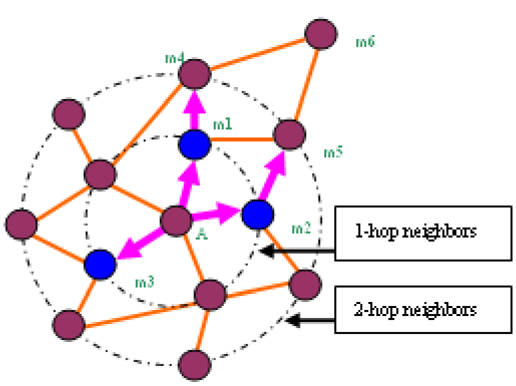

FIGURE 2.7: Re-emitting rule

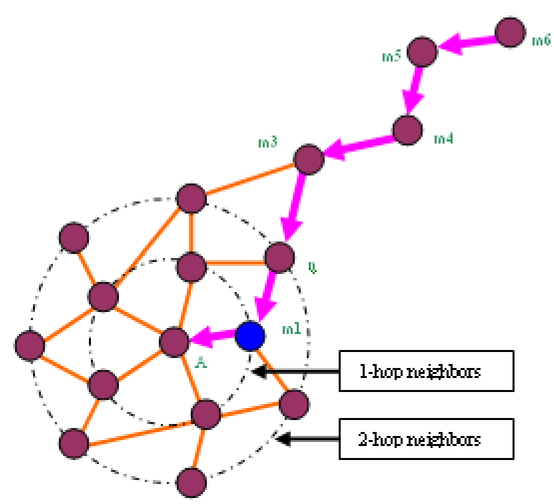

FIGURE 2.8: The shortest path with MPR link

TOPOLOGY ADVERTISEMENT IN OLSR

The MPR links are flooded in every node. Every node is able to compute the shortest path routes to every destination. On the other hand classical link state protocols will flood entire neighbourhoods, consuming additional bandwidth for just getting redundant routes.

A) MULTIPOINT RELAYS SELECTION

The objective of MPR selection is for a node to select a subset of its neighbours such that a broadcast message, retransmitted by these selected neighbours, will be received by all nodes 2 hops away. The MPR set of a node is computed such that it, for each interface, satisfies this condition. The information required to perform this calculation is acquired through the periodic exchange of HELLO messages, as described in section 6 in the RFC 3626. The MPR Selections algorithm that propose by RFC 3626 constructs the MPR set which includes minimum number of the one hop symmetric neighbours from which it is possible to reach all the symmetrical strict two hop neighbours. The node must have the information about one and two hop symmetric neighbours in order to start the needed calculation for the MPR set. All the exchange of information is broadcasted using Hello messages (H. Aleksandr, 2004).

B) TOPOLOGY SELECTION

The nodes that are selected as MPR need to send the topology control (TC) message in order to exchange and build topological information base. Only MPRs are allowed to forward TC messages, in which TC messages are broadcasted throughout the network. In order to advertise its own links, TC message must be sent by a node in the network. The node must send at least the links of its MPR selector set. The TC message includes the own set of advertised links and the sequence number of each message. The sequence number is used to avoid loops of the message, if the node gets a message with the smaller sequence number, it must discard the message without any updates. The node must increment the sequence number when the links are removed and added from the TC message (H. Aleksandr, 2004). When the nodes advertised, links set becomes empty and it can still send an empty TC messages for specified amount of time, in order to invalidate previous TC messages. The size of the TC message can be quite big, so the TC message can be sent in parts during some specified amount of time. Node can increase its transmission rate to become more sensible to the possible link failure.

C) ROUTING TABLE CALCULATION

The node maintains the routing table in which the routing table entries have “destination address”, “next address”, “number of hops” to the destination address and “local interface address”. “Next address” indicates the next hop node. The information can be get from the topological set (TC messages) and the local link information base (Hello messages). Therefore, any changes for the set, the routing table will be recalculated (P. Jacquet, A. Laouitti, P. Minet and C. Viennot, 2001).

2.2. MULTIPOINT RELAY (MPR COMPUTATION)

The detail description that specifies a procedure of the proposed heuristic and the terminology that used to describing the heuristic will get in RFC 3626 document for selection of MPRs. It constructs a MPR-set, which enables a node to reach any node in the symmetrical strict 2-hop neighbourhood through relaying on one MPR node with willingness that is different from WILL_NEVER. The heuristic MUST be applied per interface. The MPR set for a node is the union of the MPR sets found for each interface. The implementation of the algorithm is located in /src/mpr.c which is the mpr.c source code file was automatically installed when installing the OLSR software. All one-hop neighbours are linked to the two-hop neighbours that can be reached. Therefore, when selecting a neighbour as MPR, all corresponding two-hop neighbours can easily be updated to reflect this. The algorithm removes all previous selected MPRs and recalculates the whole MPR set. This is done by traversing the neighbour set based on the registered willingness of neighbours, starting with a willingness of 7 and decreasing down to 1. Nodes with a willingness of 0(WILL_NEVER) are never selected as MPRs wile nodes announcing a willingness of 7(WILL_ALWAYS) will always be selected as MPRs.

2.3. WILLINGNESS (SETTING WILLINGNESS)

"Willingness" is a willing or interest of the node in the Ad Hoc network to give a contribution or commitment to the other nodes in order to send a data in the network. In OLSR, willingness is set based on the power-status of the node. This information is extracted from the pseudofile /proc/apm, which is the user-space interface to the *Advanced Power Management* offered by the kernel. Advanced Power Management (APM) is the predecessor to ACPI. The BIOS needs to handle all power management which devices are being set into lower power status based on the device activity timeouts. In this case, if no such file is present, willingness will be set to WILL_DEFAULT (3). The user can also set a fixed value for willingness in the configuration file. The willingness is based on a trivial calculation. Beneath is the snippet of code that calculates willingness. This code is implemented in the function "olsr_calculate_willingness" in src/olsr.c. This olsr.c source code file was installed automatically into the nodes computer when doing the installation of the OLSR software.

```
/* If AC powered */
if(ainfo.ac_line_status)
  return 6;

/* If battery powered
 *
 * juice > 78% will: 3
 * 78% > juice > 26% will: 2
 * 26% > juice will: 1
 */
return (ainfo.battery_percentage / 26);
```

FIGURE 2.9: Source code for "olsr_calculate_willingness" function in olsr.c source code file

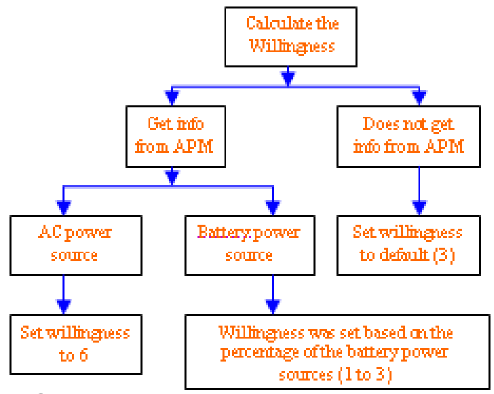

FIGURE 2.10: The willingness calculation flow diagram

2.4. OLSRD PLUG-IN

In order to maintain the communication session, process and generate packets, OLSR allows the usage of dynamically linked plug-ins, which is able to access the necessary functionality in it. Plug-ins can be used for almost everything because the plug-in interface offers a multi-purpose call to perform its specialized tasks. The OLSR daemon (olsrd) is support dynamic loading of plug-in (dynamic link library) for generation and processing of private package type starting from the version 0.4.3. The OLSR version that we used on the experiment was version 0.4.10. The design has been chosen because it does not need to change any code in olsrd in order to add custom package of functionality. The plug-in also can be written with any languages that can be compiled as a dynamic library. Thus, a person does not need to use the extended OLSR functioning to rely on heavy patching in order to maintain functionality whenever the new olsrd version is released.

2.5. THE POWERSTATUS PLUG-IN

The powerstatus plug-in provides a function where the node periodically floods the network with a custom packet, containing the following information:

- Whether or not the node is battery powered
- Estimated usage time left on the battery if using a battery
- Percentage of power left on the battery if battery powered.

It is very useful to inform the other nodes about the status of the power info itself. This information is very useful for the node to calculate the willingness for the usage of the other node to select a MPR. The details about the MPR and willingness have been discussed earlier of this chapter.

3.0 METHODOLOGY

3.1. RESEARCH TOOLS

We use specific tools for doing the experiments such the operating system, hardware, software and also the environment of the testbed. We need to verify the specific tools because the different tools that we used sometimes give some effect to the result that we collect. It is also important because we need to make sure that all the element that we used for the tools are applicable and can work well without any error.

3.1.1.OPERATING SYSTEM REQUIREMENTS

The platform used Linux operating system (Fedora Core 5 and 6) in the experiment because the updated development of OLSR was created on it. In order to make sure the OLSR software could work with the latest Linux operating system, the latest version of Linux was chosen for experiment ensuring the required capabilities. Thus, the latest Linux kernel version (version 2.6.19) was used in the experiments ensuring that the results from the experiments are reliable.

3.1.2.HARDWARE REQUIREMENTS

In order to achieve greater mobility, wireless notebook devices were used to perform the OLSR functions. Other devices such as PDAs or hand phones are also suitable with OLSR depending on the operating system that supports the hardware. For this testbed, three DELL's notebooks Latitude D500 named as Telco1, Telco2 and Telco3 are been used. Another notebook that has been used in the experiment was Acer Aspire 5580, which was given the name Acer. The detail of the specifications and configurations is shown in TABLE 3.1.

	Dell Latitude D500	**Acer Aspire 5580**
Processor	Intel Pentium M Processor 100 MHz	Intel Core 2 Duo Processor 1.66 GHz
Memory	256 MB RAM	512 MB RAM
Storage	40 GB HDD	80 GB HDD
Network Adapter	• Intel Pro/100 VE Network Connection • Intel Pro/Wireless LAN 2100 3A Mini PCI Adapter	• Intel PRO/Wireless 3945ABG Network Connection • Marvell Yukon 88E8038 PCI-E Fast Ethernet Controller
Operating System	• Windows XP Pro • Fedora Core 5/6	• Windows XP Home • Fedora Core 6
Other Device	• CDRW Drive	• COMBO Drive • Bluetooth

TABLE 3. 1: The hardware specification and configuration for OLSR nodes.

3.1.3. SOFTWARE REQUIREMENTS

The experiments used the latest version of the OLSR in the implementation of the testbed utilizing the olsrd-0.4.10 version. There are a lot of enhancements in OLSR, entailing the use of the latest version that is free from bugs compared to the previous version. Therefore, the latest version is better and more reliable for use in the experiment owing to its latest features of OLSR software. The 'gcc' (gnu c compiler) is one of the prerequisite software for the OLSR that should be installed in the Linux for OLSR software compilation. Others software or tool the used was wireshark software, ping and traceroute or tracert tools.

3.1.4. TESTBED REQUIREMENT

This experiment was tested on MUST campus environment, which involved the first floor and second floor of wing C comprising the Wireless room, IT lab, library and the corridor in the first and second floor for testbed. The results would differ if the experimental requirements chosen were altered.

3.2. OLSR SOURCE CODE MODIFICATION

The focus of the experiment is on maximizing the battery usage and the OLSR performance namely the modification of the core and the power status plug-in on the OLSR software to determine the change of willingness that relate to the usage of power resources based on the AC power or battery power sources. At this juncture, the willingness can be enhanced and upgraded in order to maximize the usage of the resources especially when the node is using the battery power sources. FIGURE 2.11 in Chapter 2 summarizes the flow of the willingness calculation, which includes the Core OLSR function and the power status plug-in on OLSR. In the basic OLSR core, only the default and manual willingness setting for the node itself is available. On the other hand, the power status plug-in is where the willingness calculations are performed. The plug-in also has the function as the source of the power information that will be broadcasted into the network where the information will be picked by other node in order to know the power status of the other nodes.

The default value that is set in the core OLSR implementation is 3 because the information from the /proc/apm file is not available. The node may use the power source either using the AC or battery power. In this case, other nodes could not know the status and information about the node and for safety purpose; the willingness is set to the value of 3 because if the node uses the weak battery power, the network would automatically lose it without any warning invariably affecting the network to lose data. Alternatively, the setting can be based on user needs if they do not want to install power status plug-in with set the willingness to default or set the value (1-3 value) at the olsrd.conf file in order to allow the information for the node of the power status known to other devices. The willingness calculation on the other hand is located at the power status plug-in. The information flows to the power status plug-in function and then it will be calculated. The value of the willingness will be calculated when the usage of the AC power sources is 6. While the willingness value 1-3 indicating the percentage of balance of the battery power source. The values that have been calculated are not efficient because the resource is not consumed maximally. However, it has to maximize the usage of the power sources particularly in emergency situations such as natural disaster, fire, and earthquake and also for the military operations.

Therefore, it is proposed that the value is change from 6 (old willingness value) to 7 (new willingness value) when using AC power because the source can get the power consistently. When using the battery power source, the value change from 1 - 3 (old willingness value) to 0 – 7 (new willingness value), thus increasing the granularity of the possible values and maximizing the resources available to the nodes. The main reason for optimizing the power resource and willingness are to make sure all nodes have enough battery power resource in which the battery is limited and it have more chances to be selected as MPR. The details of the MPR are summarized in the FIGURE 3.1 below.

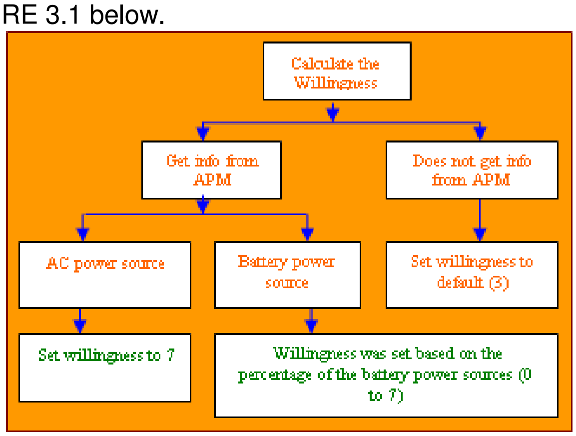

FIGURE 3.1: The new value for the willingness calculation flow diagram

3.3. OLSR INSTALLATION WITH POWER STATUS PLUG-IN SOFTWARE.

In default, the willingness value is automatically derived from the core OLSR software without the calculation of the willingness. However, it does not use the power status information from the /proc/apm file. It only uses either the default value that have been set or the value from the user setting. The willingness calculation function is located at the power status plug-in where the plug-in is not installed by default with the OLSR software during the installation. The power status plug-in should be installed manually when the user needs to optimize power utilization with OLSR. The OLSR software can work well if the power status plug-in is not installed and A/C power is used, but the results of such OLSR experiments are not highly reliable because it does not replicate the real situation. In real ad hoc network, sometimes there is no infrastructure and it needs the power status function to calculate the willingness based on the information from the /proc/apm file [8].

4.0 SETUP AND INSTALLATION

4.1. INTRODUCTION

The OLSRd software started out as part of the Master thesis project for Andreas Tonnesen at the University Graduate Centre. The OLSRd project is still on-going while the Master thesis has reached its completion. All nodes must be capable to detect and communicate with each other to establish a network where the infrastructure does not exist or where the services are not required. The IEEE 8102.11 Ad-hoc mode does not support multihop communications, whereas OLSR does. In the OLSR testbed, the Acer node could talk to Telco3 node through Telco2 node where the Acer node and Telco3 node were out of range (radio). The FIGURE 4.1 illustrates the testbed implemented in the experiment.

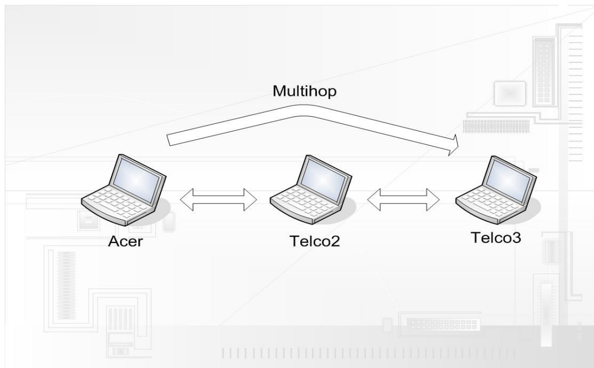

FIGURE 4.1: Multihop on OLSR

4.2. OLSR INSTALLATION

The nodes of the OLSR testbed were setup using Fedora Core 5 and Fedora Core 6 with the latest update kernel 2.6.19. It involved four notebooks that were installed with the OLSR software. The OLSR software can be downloaded through the internet at **www.olsr.org** web site. The source files were tarred using tar and bzipped using bzip2. This experiment used the release source which was 0.4.10. Then, after extracting the file, it was compiled and installed after browsing and achieving it. After the compilation and installation was complete, the olsrd.conf file, which is located at /etc/olsrd.conf was configured. All nodes are configured with the static IP address (and they must be, since there is no DHCP server to provide a dynamic address).

4.3. NETWORK CONFIGURATION ON OLSR

OLSR nodes must get the latest update kernel of the Linux operating system (Fedora Core 5 and 6) from the ftp site and it also must been installed with gcc. The gcc in Linux is used to compile the source code after performing the changes of the OLSR source code. The wireless interface on each node should be configured with an IP address. The nodes should be configured with the same ESSID. The wireless card should be configured with “ad-hoc” mode. The other thing that is compulsory is to release the UDP/698 from blocking. When all the networks have been configured, the next step is to configure the **olsrd.conf** file. The main option that has to change is the debug level (0 – 9) which can be seen through the process where the daemon runs. Next is the IP version, and in this case it uses IPv4. Lastly, it will configure the wireless interface under the name “eth1”. More details about the configuration can be found in the olsrd.conf document. The configuration can be enhanced depending on the needs of a user. The basic configuration needs on the olsrd.conf file is shown in Figure 4.2. The interfaces for the wireless are different for each other ensuring that the interface, which was already set at the olsrd.conf file, is correct. Then, the interface could be checked by using the command code at the terminal windows. Therefore, the tests that were planned performed well representing a small scale of the network (FIGURE 4.3).

```
Acer / Telco 1 / Telco2 / Telco3
/etc/sysconfig/network_scripts/ifcfg-eth1
…
MODE=Ad-Hoc
ESSID=olsr
CHANNEL=1
RATE=11M

/etc/olsrd.conf
DEBUG          3
IPVERSION      4
…
INTERFACE  "eth1"
{...
Ip4Broadcast             255.255.255.255
…}
```

FIGURE 4.2: The network configuration and olsrd.conf file for OLSR nodes.

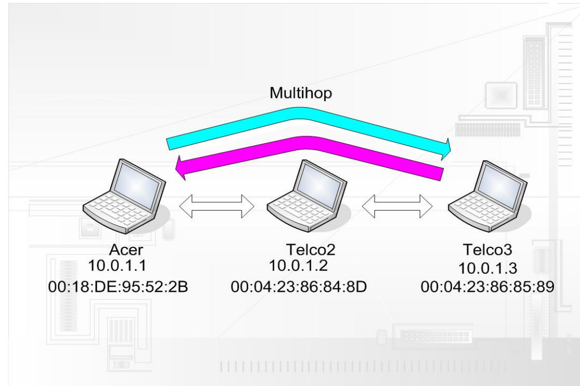

FIGURE 4.3: OLSR network communicate

On the other hand, the OLSR network can also be connected to the hard-wired (Ethernet) connection for a large network as well as network interface running on OLSR. It uses the Node and Network Association (HNA) message that contains sufficient information for the recipients to construct an appropriate routing table enabling the HNA (for IPv4 or IPv6) in the olsrd.conf file (FIGURE 4.5). FIGURE 4.4 illustrates the OLSR connection with the large fix connection.

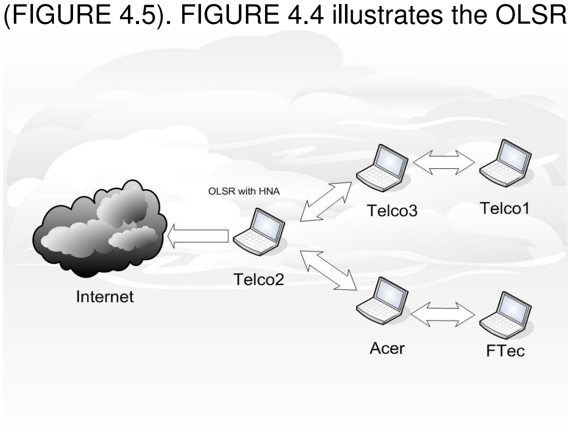

FIGURE 4.4: OLSR connection with large fix network.

```
Acer / Telco2 / Telco3
/etc/olsrd.conf
DEBUG          3
IPVERSION      4
…
Hna4
{
 …
}
…
INTERFACE  "eth1"
{
...
Ip4Broadcast             255.255.255.255
…
}
```

FIGURE 4.5: The HNA configuration on olsrd.conf file.

4.4. INSTALLATION THE PLUG-IN ON OLSR

The OLSR nodes were actually connected to each other without knowing the power status of the default node. It is actually optional for the OLSR to work without the power status function. In this experiment, the power status plug-in that has been provided with the OLSR source code file would be used during the downloading and installing process into the nodes. On the other hand, this function was not installed into the node when installing the OLSR automatically. Hence, it must be installed manually because it is optional for the OLSR as it is not a core function. The Power Status plug-in locates the *olsrd library* directory when the OLSR is installed into the computer. It uses the **Make** and **Make Install** commands to compile and install the power status function. When the compilation and the installation of the OLSR are complete, it must configure the olsrd.conf file as shown in Figure 4.6 below.

```
/etc/olsrd.conf
DEBUG           3
IPVERSION       4
…
LoadPlugin "/usr/lib/olsrd_power.so.0.3"
{
}
…
INTERFACE  "eth1"
{...
Ip4Broadcast            255.255.255.255
…}
```

FIGURE 4.6: Adding the plug-in script olsrd.conf file

The "olsrd_power.so.0.3" would be located at the /usr/lib/ after the power status installation. It should be located at the correct path because it would show the error and the OLSR automatically terminates (stops) when it runs the OLSR. It must also have the open and close curly bracket after the plug-in function. Once completed, the OLSR network should be tested to determine whether an error has occurred or not.

5.0 NETWORK ANALISYS

When all the modifications were completely compiled, we next tested the resulting version on the network and collected some result from the OLSR deployment. The data collection only focuses on the availability of the nodes and also on the routing of the nodes on the ad-hoc network. This is because, the focus of the modification is to make sure the node on the OLSR is selected as MPR and to make sure the node is transferring the data willingly on the ad-hoc networks by using the limited battery power sources. Theoretically, the original OLSR source is calculating the percentage of the battery power balance and the willingness that can be acquired as summarized in FIGURE 5.1 and the modification of the OLSR source is summarized in FIGURE 5.2 as below.

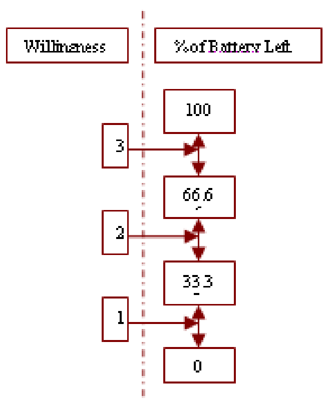

FIGURE 5.1: The percentage (%) of battery power balance with the willingness assign (original source)

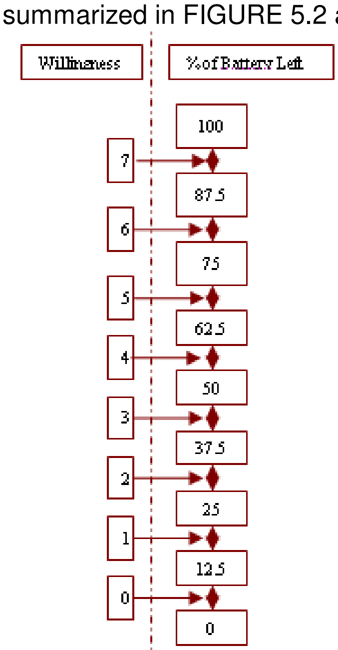

FIGURE 5.2 : The percentage (%) of battery power balance with the willingness assign (modification source)

Based on FIGURE 5.1 and FIGURE 5.2, comparison of the "Willingness" between the sources is illustrated in TABLE 5.1. The "Willingness" value based on the percentage (%) of battery power left is shown in Figure 5.7.

% of Battery Left	Willingness for Modify Source	Willingness for Original Source
100	7	3
90	7	3
80	6	3
70	5	3
60	4	2
50	4	2
40	3	2
30	2	1
20	1	1
10	0	1
0	0	0

TABLE 5.1: The willingness comparison table between original and modification sources

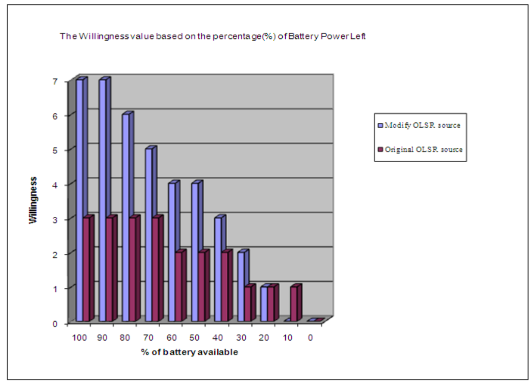

FIGURE 5.3: The comparison table on the willingness for original and modification sources based on the percentage of battery power left.

FIGURE 5.3 shows that the willingness for the modified source code is better than the original source code until the percentages of the battery power available reached 20% level. Then, the percentages of battery dropped from 12.5% to 0%, where the “Willingness” was set to 0, in order to give the node enough time to shutdown properly saving all the works being performed. TABLE 5.1 and FIGURE 5.3 show that the “Willingness” on the OLSR plays an important role in choosing a node as MPR.

OLSR availability

During the experiment on the OLSR ad-hoc network, the network itself must be available. It will affect the OLSR ad-hoc network if the nodes on that network were not available. It will also become a major factor in the measurement performance for the OLSR ad-hoc network. To test the availability of the nodes, “Ping” is used to check either the nodes are available or not on the network. In this experiment, four notebook computers were used for checking the OLSR availability. The details on the hardware and software specifications have been discussed in CHAPTER 3, in which the nodes setup is illustrated in FIGURE 5.4 overleaf.

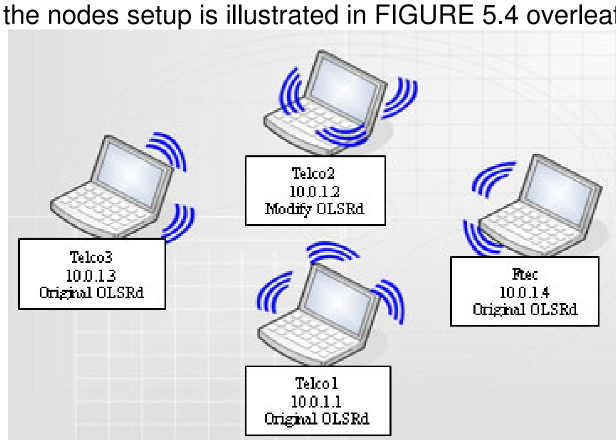

FIGURE 5.4: OLSR networking topology

5.1. USING AVAILABILITY STATISTIC DURING OLSR EXPERIMENT

When multiple ping packets are sent to a remote node, the ping program tracks on how many responses are received. The result will display as the percentage of the packets, which is not received. A network performance tools can use the “ping” statistic to obtain basic information regarding the status of the networks between the two end points. Once it is confirmed that there are lost packets in the “ping” sequence, it must determine the cause of the packet loss either due to the collisions on network segment or the packet being dropped by a network device. In the experiment, there was no packet loss on the OLSR networks.

5.2. ROUTING TABLE

When the network in all the OLSR nodes were available and all of them were communicating each other, the Telco3 node then moved far away from Ftec node until the node was out of range of the Ftec node. This is because the Telco3 node must use either the Telco1 or the Telco2 node in transferring the data to the Ftec node and vice versa. In the experiment, the setup of the nodes was performed as illustrated in FIGURE 5.16.

1. Ftec node (10.0.1.4) was located at the wireless room in the IT lab. Telco2 node (10.0.1.2) and Telco1 node (10.0.1.1) were located in the IT Lab near the door. All the three nodes were on the first floor situated on the left side of Wing C.
2. Telco3 node (10.0.1.3) was located on the second floor, in front of the lecture rooms, which was far away from Ftec node (10.0.1.4). Both nodes were out of line-of-sight range from one another. In this case, both nodes could only communicate via Telco1 or Telco2 node.

However, it needed to collect the data for analysis from the routing table for Ftec node and Telco3 node using a “traceroute” for Fedora Core 5 and “tracert” for Fedora Core 6. This experiment was performed based on time frame to get better result. The result shows that the Ftec node (source node) chose Telco2 node to transmit the data to the Telco3 node (destination) and the Telco3 node (source node) chose Telco2 node to transmit the data to Ftec node (destination node). Therefore, Telco2 node was selected as MPR because the value of the willingness was higher than telco1.

5.3. SUMMARY FROM THE EXPERIMENT

The result shows that the willingness plays an important role in choosing a node as MPR in OLSR Ad Hoc network. The higher value of the willingness of the node, the more possibility of that node to be chosen as MPR. The lower value of the willingness of the node, the lower the possibility of the node to be chosen as MPR. On the other hand, if all nodes have almost the same of the less value, then the MPR will be chosen according to the highest value among the nodes. However, the results will be different if the experiment involves more nodes and in different situations. There are also other factors that can generate different outcomes such as the distance between the nodes, the barriers in term of the radio frequency from the buildings, thick walls, mirrors, doors and others. In conclusion, the experimental results provide evidence that enhancing the facilities of OLSR by creating new scheme on calculating the willingness; it will create more paths in the network for the node to choose the shortest path to the destination eventhough the battery power resource is limited.

6.0 DISCUSSION AND CONCLUSIONS

6.1. OLSR Installation

Several important aspects need to be addressed when the OLSR network on the Fedora Core 5 and Fedora Core 6 as revealed in the experiment. The wireless adapter must be properly installed and fully functioning to ensure smooth data transmission. The latest kernel version for the system has to be put in place with the essential software to run the OLSR namely gcc for compiling and GTK2.0 development libraries to compile the GUI front-end. The wireless network configuration has to change from the “managed” mode change to “ad-hoc” mode and the setting of the ESSID, CHANNEL and RATE must be performed in accordance with the new setup. Testing for compatibility with Linux Fedora Core 5 and 6 and also other requirements need to be performed in the installation of OLSR using the third party sources. A complete documentation for the OLSR network development on different platform is essentially to help developers or researchers to setup their OLSR network easily and effectively. Currently, there is no OLSR for Windows that works on IPv6. The third party software for OLSR did not perform very well such as the PDA device like iPAQ, which is a run under the Windows Operating System like Windows Mobile 5.0.

6.2. LIMITATION

There are some limitations in the experiment conducted. The preparation of the OLSR platform needs each node to be wireless. The experiment was prepared for mobile ad-hoc network nodes requiring the deployment of at least four nodes, which were divided into 3 parts. First, it needs one source node, one destination node and at least two nodes in the middle network. The more nodes used for the experiment, the better results obtained in making comparison with networks having less nodes will shows of that network in which it can find the disadvantages from that networks. It was quite difficult to get sufficient mobile nodes (notebooks) when performing the experiment due to the prohibitive cost. To fulfill the minimum requirements, available devices of the researcher and borrowed devices were used.

REFERENCES

1. C. Guillaume, & Eric F. (2002). *Ananas: A New Ad hoc Network Architectural Scheme.* INRIA Research Report – 4354.
2. Aleksandr H. (2004). *Comparing AODV and OLSR Routing Protocols.* Telecommunication Software and Multimedia Laboratory, Helsinki University of Technology. Sjokulla.
3. Laoutti, Muhlethaler P., Najid A.,& Plakoo E. (2002). Simulation Results of the OLSR Routing Protocol for Wireless Network. *1st Mediterranean Ad-Hoc Networks workshop (Med-Hoc-Net).* Sardegna, Italy.
4. Viennot L. (1998). *Complexity Results onElection of Multipoint Relays in Wireless Networks*. Technical Report, INRIA.
5. Jacquet P., Laouitti A., Minet P., & Viennot L. (2001). Performance Analysis of OLSR Multipoint Relay Flooding in Two Ad-Hoc Wireless Network Models. Research Report – 4260. *RSRCP Journal Special Issue on Mobility and Internet*. INRIA.
6. Jacquet P., Minet P., Muhlethaler P., Rivierre N. (1996). *Increasing Reliability in Cable Free Radio LANs: Low Level Forwarding in HIPERLAN*. Wireless Personal Communications.
7. Andreas T. (2004). *Implementing and Extending the Optimized Link State Routing Protocol.* Department of Informatics, University of Oslo. Oslo.
8. Clausen T., Jacquet P. (2003). Request for Comment: 3626. *Experimental Project Hipercom.*

Improved Irregular Augmented Shuffle Multistage Interconnection Network

Sandeep Sharma sandeep_gndu@yahoo.com
Department of Computer Science & Engineering
Guru Nanak Dev University, Amritsar, 143001, India

Dr. K.S.Kahlon karanvkahlon@yahoo.com
Department of Computer Science & Engineering
Guru Nanak Dev University, Amritsar, 143001, India

Dr. P.K.Bansal principalmimit@yahoo.com
MIMIT College of Engineering and Technology,
Malout , India

Dr. Kawaljeet Singh
directorucc@pbi.ac.in
Computer Centre
Punjabi University, Patiala, 143001, India

Abstract

Parallel processing is the information processing that emphasized the concurrent manipulation of data elements belonging to one or more processors to solve a single problem. The major problem to achieve high-level parallelism is the construction of an interconnection network to provide interprocess communication. One of the biggest issues in the development of such a system is to developed fault tolerant architecture and effective algorithms to analyze its characteristics. An irregular class of Fault Tolerant Multistage Interconnection Network (MIN) called Improved Irregular Augmented Shuffle Network (IIASN) is proposed. The characteristics of some popular irregular class of Multistage Interconnection Networks along with proposed IIASN network which is based on IASN[11] Network are also analyzed in this paper.

Keywords: Augmented Shuffle Network (IASN); Fault Tolerant MIN; Four Tree Network; Multistage Interconnection Network; Routing; Permutation.

1. INTRODUCTION

In the era of parallel processing the multistage interconnection networks are frequently projected as connections in multiprocessor systems to interconnect several processors with several memory modules or processors. A multistage network is capable of connecting an arbitrary input terminal to an arbitrary output terminal [8]. In general a typical MIN consists of more than one stage of small interconnection networks called switching elements (SEs)[10][2]. The stage and number of switching elements may vary from network to network. There are many parameters like path length, cost, and permutation passable that are deciding factor for the whole system performance [9]. In this paper an irregular class of multistage interconnection network named

IIASN is designed and analyzed. This paper organized as follows: Section 2 describes the construction procedure of proposed network. Section 3 provides a brief introduction to cost effectiveness and its analysis. Section 4 discuses the path length analysis of various networks along with proposed network. Section 5 describes the permutation passable analysis of some popular MINs. Finally conclusions are given in Section 6.

2. CONSTRUCION PROCEDURE OF IIASN NETWORK

A typical IIASN is an Irregular Multistage Interconnection Network of size $2^n \times 2^n$ is constructed with the help of two similar groups; lower and upper, each group consisting of a sub network of $2^{n-1} \times 2^{n-1}$ size and has 2^{n-2} –1 stages, both stages at $\log_2 N - 3$ and $\log_2 N - 1$ have 2^{n-1} switches (where $N=2^n$ of N x N network). The centre stage has exactly 2^{n-3} switches. The switches in the first stage form a loop to provide multiple paths if a fault occur in the next stage. Each source is connected to two different switches in each group with the help of multiplexer and each destination is connected with demultiplexer. In case the main route is busy or faulty, requests will be routed through alternate path in the same sub-network. The advantage of this network is that if both switches in a loop are simultaneously faulty in any stage even then some sources are connected to the destinations. IIASN network of size 16x16 is illustrated in Figure 1.

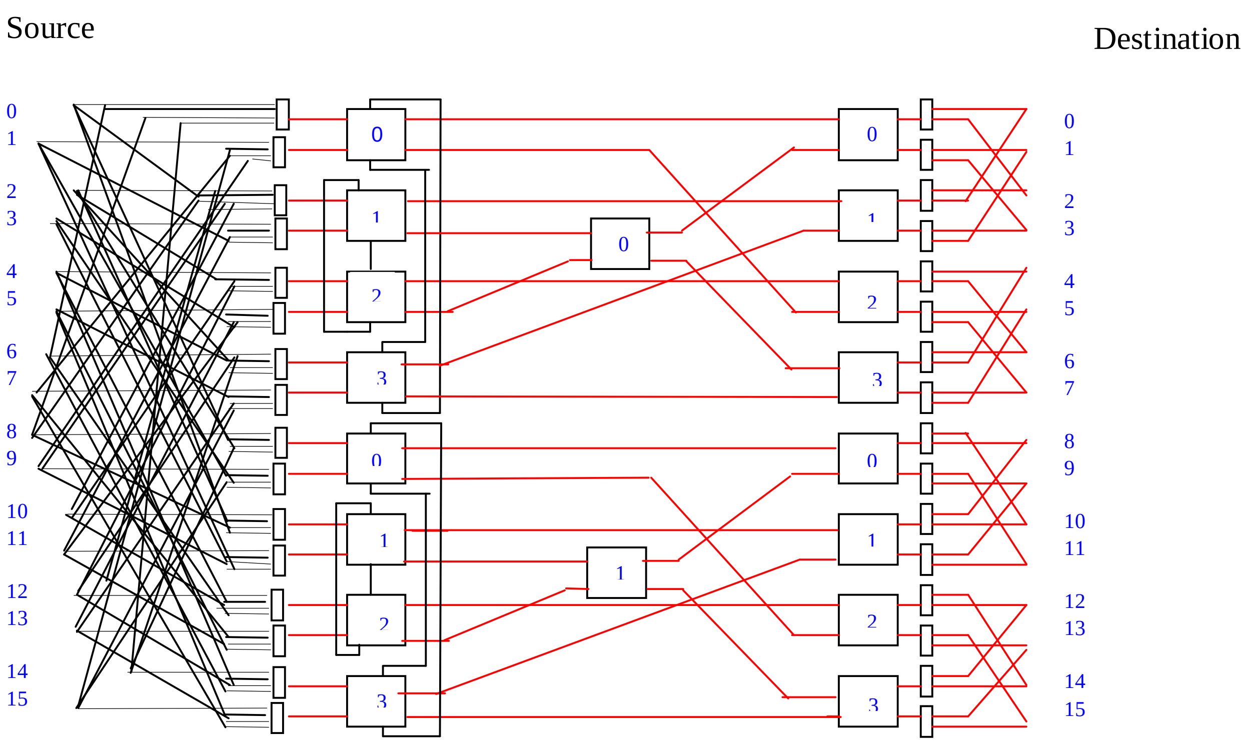

FIGURE 1: IIASN MIN of size N=16

3. COST-EFFECTIVENESS ANALYSIS

A common method is used to estimate the cost of a network that is to calculate the switch complexity with the assumption that the cost of a switch is proportional to the number of gates involved, which is roughly proportional to the number of 'cross points ' within a switch [1][10]. So in this way the cost of n x n switch comes out to n^2. For an interconnection network that contains multiplexers and demultiplexers, it is roughly assumed that each Mx1 multiplexers or 1xM demultiplexers has M units.[3] . Hence the cost of IIASN network is

Total number of 3x3 switches = 2^{n-1}
Total number of 2x2 switches = $2^{n-1}+2$
Total number of multiplexer $=2^{n}$
Total number of demultiplexer $=2^{n}$
Overall cost of network is = 208

Network	**Cost**
IIASN	208
IASN	236
FT	258
MFT	276

TABLE 1: Cost comparison of various networks

4. PATH LENGTH ANALYSIS

Path length refers to the length of the communications path between the source to destination. Multiple paths of different path lengths are possible in a network .It can be measured in distance or by the number of intermediate switches. The possible path lengths [4] between a particular pair of source to destination may vary from 2 to maximum number of stages. The various path lengths of some popular networks along with proposed network is calculated to route a data from given source (let S=0 i.e 0000) to all destination is shown in table 2.

<table>
<tr><th>Source</th><th>Destination</th><th>Path length of IIASN</th><th>Path length of IASN</th><th>Path length of FT</th><th>Path length of MFT</th></tr>
<tr><td rowspan="16">00000</td><td>0000</td><td rowspan="16">2,3</td><td rowspan="4">2,3</td><td rowspan="2">2,4,5</td><td rowspan="2">2</td></tr>
<tr><td>0001</td></tr>
<tr><td>0010</td><td rowspan="2">4,5</td><td rowspan="6">5</td></tr>
<tr><td>0011</td></tr>
<tr><td>0100</td><td rowspan="4">3</td><td rowspan="4">5</td></tr>
<tr><td>0101</td></tr>
<tr><td>0110</td></tr>
<tr><td>0111</td></tr>
<tr><td>1000</td><td rowspan="4">2,3</td><td rowspan="2">2,4,5</td><td rowspan="2">2</td></tr>
<tr><td>1001</td></tr>
<tr><td>1010</td><td rowspan="2">4,5</td><td rowspan="6">5</td></tr>
<tr><td>1011</td></tr>
<tr><td>1100</td><td rowspan="4">3</td><td rowspan="4">5</td></tr>
<tr><td>1101</td></tr>
<tr><td>1110</td></tr>
<tr><td>1111</td></tr>
</table>

TABLE 2: Comparison of path lengths of IIASN and other networks

5. PERMUTATION PASSABLE ANALYSIS

Permutation [6] is the one to one association between source to destination pair [7][5]. Path length and the routing tags parameters are the major backbone to evaluate the permutation. There are two ways to evaluate the permutation:

Identity Permutations

A one-to-one correspondence between same source and destination number is called Identity Permutation. For example correspondence between 0..0 , 1..1 and so on .In terms of source and destination this can be expressed by:

$$\boxed{S_i = Di}$$

Where i = 0,1…….N-1

For example: connectivity between source to destination for identity is represented by:

S_0 - D_0 , S_1 – D_1 ,------------------------ S_{15} - D_{15}

Incremental Permutations

A source is connected in a circular chain to the destination in incremental permutation as shown below:

S_0 – D_4 , S_1 – D_5 ,------------------------ S_{15} – D_3

We are considering the best possible cases to find out the permutations

- Non-Critical Case : If a single switch is faulty in any stage
- Critical case : If the switches are faulty in a loop in any stage (if it exists)

Permutation evaluation requires the path length of given source to destination (path length can be more than one, from a given source to destination if multiple paths exists) and the routing tags. The analysis of some popular network from given source to destination to evaluate incremental (S0 to D4, S1-D5...) permutations along with proposed network is as follows.

Stage	**Switch / Faults**	**Total path length**	**Total no of request passes**	**Average Path Length**	**(%)passable**
	WITHOUT	30	13	2.3	81
	MUX	30	13	2.3	81
1	S0 / A	26	11	2.36	68
	S0 / B	24	10	2.4	62
2	S0	24	11	2.18	68
3	S0	25	11	2.27	68
	DEMUX	30	13	2.3	81

A – Non critical B – Critical Case

TABLE 3: Incremental permutation measures of IIASN

Stage	Switch / Faults	Total path length	Total no of request passes	Average Path Length	(%) passable
	WITHOUT	28	11	2.5	68
	MUX	28	11	2.5	68
1	S0 / A	26	10	2.6	62
	S0 / B	21	8	2.6	50
2	SA /A	25	10	2.5	62
	SA/B	19	8	2.3	50
3	S0	26	10	2.6	62
	DEMUX	28	11	2.5	68

TABLE 4: Incremental permutation measures of IASN

Stage	Switch / Faults	Total path length	Total no of request passes	Average Path Length	(%) passable
	WITHOUT	20	4	5	25
	MUX	20	4	5	25
1	S1 / A	20	4	5	25
	S1 / B	20	4	5	25
2	S2 / A	15	3	5	18
	S2 / B	10	2	5	12
3	S3 / A	10	2	5	12
	S3 / B	0	0	0	0
4	S4 / A	15	3	5	18
	S4 / B	10	2	5	12
5	S5	20	4	5	25
	DEMUX	20	4	5	25

TABLE 5: Incremental permutation measures of FT

Stage	Switch/Faults	Total path length	Total no of passes	Average path length	(%) passable
	WITHOUT	40	8	5	50
	MUX	40	8	5	50
1	S1 / A	35	7	5	43
	S1 / B	30	6	5	37
2	S2 / A	30	6	5	37
	S2 / B	20	4	5	25
3	S3 / A	30	6	5	37
	S3 / B	20	4	5	25
4	S4 / A	30	6	5	37
	S4 / B	20	4	5	25
5	S5	35	7	5	43
	DMUX	40	8	5	50

TABLE 6: Incremental permutation measures of MFT

6. CONCLUSION

An irregular class of Fault Tolerant Multistage Interconnection Network called Improved Irregular Augmented Shuffle Exchange Network has been proposed and analyzed. It has been observed from table 1 that IIASN has lesser cost in comparison to existing irregular fault tolerant networks. It has been also analyzed from table 2 that IIASN has unique and better path length in comparison to IASN and other popular irregular networks. . It has been also observed from the analysis that the permutation passable of IIASN is much better that existing IASN, FT and MFT networks.

7. REFERENCES

[1] Algirdas Avizenis, "Towards Systematic Design of Fault-Tolerant Systems", IEEE Computer, Vol. 30, No. 4, , pp. 51-58 , April 1997

[2] Patel,J.H., "Performance of processor-memory interconnection for multiprocessors." IEEE Transaction on computers , 30,pp. 771-780,1981.

[3] P.K.Bansal, K. Singh, R.C. Joshi, and G.P. Siroha, "Fault tolerant Augmented Base Line Multistage Interconnection Networks" , IEEE TENCON pp. 205-208,1991.

[4] P.K.Bansal, K. Singh, and R.C. Joshi, "Routing and path length algorithm for a cost-effective four-tree multistage interconnection network", International Journal of Electronics, Vol. 73, pp. 107-115,1992.

[5] Sandeep Sharma, P.K.Bansal, "A new fault tolerant Multistage Interconnection Network ", IEEE TENCON'02 , vol 1 , pp 347-350,2002.

[6] Shirakawa Isao, "Some comments on Permutation Layout", IEEE on Networks, Vol. 10, pp. 179-182,1980.

[7] Y.Yang,J.Wang , Y.Pan , " Permutation capability of optical multistage interconnection network ", Journal of parallel and Distributed computing " , pp.60,2000.

[8] George, B.A., P.A. Dharma and H.J. Seigel, 1987. A survey and comparison of fault-tolerant multistage interconnection networks ,Computer, vol. 20, no. 6, pp. 14-27, Jun., 1987.

[9] Park, J.H., 2006. Two-dimensional ring-Banyan network: A high-performance fault-tolerant switching network. Elect. Lett., IEEE , vol. 42,249-251,2006.

[10] Bataineh, S.M. and B.Y. Allosl,. Fault-tolerant multistage interconnection network. J. Telecomm. Syst., 17, pp. 455-472,2001.

[11] Harsh Sadawatri , P.K Bansal Fault Tolerant Irregular augmented Shuffle Network, Proceedings of WSEAS International conference on Computer Engg. And Application, January 17-19, pp. 7-12, 2007

Hybrid Optimization of Pin type fixture Configuration for Free Form Workpiece

Afzeri, Nukhaie Ibrahim afzeri@iiu.edu.my
Department of Manufacturing and Materials Engineering,
International Islamic Univ. Malaysia (IIUM),

Abstract

This paper presents an automatic mechanism using pin type fixture for holding a workpiece during machining process. The hybrid optimization algorithm is introduced to obtain the optimum configuration of pin type fixture. Combination between Genetic Algorithms (GAs) and Particle Swarm Optimization (PSO) algorithms is enable to determine optimum clamping respect to minimum workpiece deformation. Spherical type pin fixture with array arrangement in two opposite side comforms geometry of workpiece through with two supporting action. Deformation as efect of clamping force and friction slip are predicted by simulation of pin-workpiece clamping model and analyzed by Finite Element methods. Maximum deformation and slip condition are evaluated by building the parametric script of the model. Parameters of the model is assigned by the algorithm through iteration process. Satisfies clamping arrangement to minimize the deformation and prevent the slip is evaluated using GAs to arrange the pin configuration. PSO is further applied based on the result of GAs for obtaining global optimum of objective function. Result of the evaluation shown that the optimization using two algorithms could achieve the beter position and clamping configuration for variety of workpiece geometry modeled using CAD software.

Keyword: Optimization, Pin Fixture, Genetic Algorithm, Particle Swarm Optimization, Finite Element

1. INTRODUCTION

Selection of best fixture for holding variety of workpiece geometry is tending to time consuming and costly. Pin type fixture is an alternative for free form geometry where only single fixture for many workpiece design. Reconfigurable fixturing is becoming a necessary component in order to reduce the cost of fixture development. Comparing to the development of new fixturing system, pin type fixture have possibility to reduce the production cost significantly especially for low repetitive machining. Various geometry of the parts could be hold by a pin type fixture with certain clamping configuration. Pin fixture has been investigated as an attachment that used for setup free on machining process with capability to hold variety of part geometry [1]. A part hold by setup free attachment could be machined completely on one process by using long round bar as raw material.

Main criteria of the fixture for holding the workpiece are should maintain the workpiece within acceptable accuracy and stability during machining process. Every point of the fixture should in contact with the workpiece. Proper workpiece holding and clamping location are important to machining quality in terms of precision, accuracy and surface finish of the part.

A simulation model through FEA tools that evaluate the performance of the pin fixture-workpiece model will help the engineers to determine the better configuration and save lead time for workpiece setup. The technique in simulation is to represent every point where the pins are in contact with the workpiece using springs element.

For a pin type fixture with array arrangement, holding of the workpiece is performed by clamping force in axial direction and friction force in tangential direction. Amount of friction force is the function of clamp in axial force and coefficient friction. Friction force should strong enough to prevent slip of the workpiece. However, increasing the friction force only can be done by increasing the clamping force which may affect to the part quality. In this paper, Finite Element modeling of pin fixture and workpiece system for evaluation of workpiece deformation and slip detection is discussed. Ansys software has been used for calculating the deflection and slip for various pin configuration and cutting forces. Spring model is used instead of pin with contact behavior for detection of slip. Parametric script file is built for accepting a variety of modeling input data.

Fig. 1 shows a prototype of array pin type fixture developed in the laboratory. There are a number of 45 pins with 10 mm diameter in one side. Two types of pins, flat and spherical type are provided for clamping the variety geometry of workpiece material. Distance between pin is 15 mm. In this paper, only presents the variation of sixteen pins.

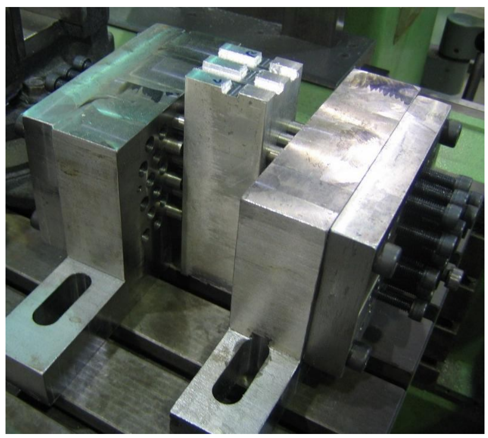

FIGURE 1: Prototype of Pin Type fixture

2. LITERATURE REVIEW

Pin type reconfigurable fixture has been considered as an alternative device for holding the irregular workpiece geometry for machining. Many researches for fixture design have been considered in recent year. Utilization of FEA for fixture modeling and simulation technique has been published in many literatures.

FEA was used as a platform for cost-effective and accurate simulation of complex dynamic fixture–workpiece behavior [2] [3]. Calculation of deflections using FEA for the minimization of the workpiece deflection at selected points as the design criterion also introduced [4]. Commercialized FEA software, Ansys, is utilized to verify fixture design integrity and the optimization analysis [5].

Genetic Algorithm is useful technique in engineering for problem solving optimization. Optimization technique using finite element modeling for analysis and verification of optimal fixturing configurations with methods of force closure also investigated [6].

Locating of clamping position using genetic algorithm has been investigated by several researchers [7] [8].

Fixture layout optimization has been implemented using Matlab GA tool and NASTRAN for Finite Element Model. Determination of optimal fixture configuration design using GA and Nastran has been applied for sheet metal assembly [9].

Most of the studies are to develop new fixture layout for new design of part where 3-2-1 approach used for the design. However, attention focused on the pin type fixture still limited where the friction slip is considered as the main holding factor. In application of Finite Element Analysis (FEA), the model to analyze a fixture–workpiece system is completely rigid [10]. In the Pin type fixture system, rigidity of the pins causes inaccuracy on clamping. For various cases, Evolutionary algorithms are not possible to obtain optimal solution. Hybrid methods are introduced in this paper in order to find the best fixturing condition.

3. METHODOLOGY OF GENETIC ALGORITHMS

GAs is an evolutionary algorithm for optimization of a system. There are several major ways for optimization technique which different that traditional gradient. Genetic Algorithm is an optimization technique work with a coding of the design variable. Many different design points are evaluated during iteration where it is a better way instead of sequentially moving from one point to the next. GA which uses probabilistic transition rule to find new design point only need a fitness as a objective function to find optimum condition. GAs approach is suitable for problem which doesn't have well defined mathematical definition between the function and variable. Evolutionary algorithms are known the best problems solution tool applied where optimality of the system difficult to be tested.

Basic procedure of GA is as following step. Firstly generate initial population of chromosome randomly. Secondly, evaluate the fitness function for each chromosome in the population. Thirdly, Satisfies condition for new generated population is then tested. Reliability of each chromosome is evaluated based of the fitness value. Forth step is generating new population by reproduction, crossover and mutation operation. Reproduction is selection of two parent chromosomes from population according to their fitness. Crossover is a probability to form a new offspring (children). Offspring will an exact copy of parent when no crossover was performed. Mutation is a probability of new spring at each locus. The last step is to use new generated population for further run of algorithm as conducted from second to fourth step.

Best value of number iterations and mutation probability has to be selected to achieve the optimum objective function. For several model cases, this value should be chosen by trial and error. In order to improve the result of GA evaluation, hybrid evaluation is utilized by combining GA and PSO. An optimal solution resulting of GA evaluation further can be processed using PSO algorithm. There are four variables are used for evaluation. Two variables for the pin left and right side and another two are workpiece position in y and z. Pins configuration for left and right side are determined by GA to the best configuration while optimum positions around the best configurations are determined using PSO algorithm.

4. CLAMPING FORMULATION

Pin type clamping fixture should satisfy the functional requirement such as centering, locating, orienting and supporting [11]. Deformation due to the clamping force influences the accuracy of the workpiece during machining. When clamp is actuated this causes the deformation error. Maximum deformation should be in the range of tolerable accumulative error. Pin type reconfigurable fixture has two side array pin with equal number in each side. One side is assigned as locator while another side as clamp. Evaluation of clamping pin is to determine the better number of pins for a setup and preventing the slip.

Pins configuration is determined base on clamping stability and deformation on a pin-workpiece model. There are two forces act to restrain the workpiece; axial clamping force and friction force. Direction of axial forces is normal to workpiece surfaces. Friction force restrains the workpiece in tangential direction with two vector directions, x_i and y_i. Pin–workpiece deflection model for spherical-tipped pins is assumed to be given by that of a spherical-tipped cylindrical punch indenting an elastic surface.

In contact pins are modeled with three springs k_{xi}, k_{yi} and k_{zi} as proposed [12]. Variables k_{xi}, k_{yi} are stiffness in tangential direction and k_{zi} is stiffness in pin axial direction. Value of spring constant (k) is dependent to the pin length which may be different for variety geometry of workpiece. Constant clamping force using hydraulic is considered during evaluation. All clamping pins are actuated with the same force. Objective function of the model is deformation of the workpiece which is evaluated by Finite Element analysis.

The contact force-displacement for a pressed spherical-tipped pin element over a curved workpiece surface is derived as follows. Spherical-tip deflection for axial and radial direction is defined as [13]:

$$\delta_z = \left[\frac{9F_a^{\ 2}}{16R(E^*)^2}\right]^{1/3} \qquad (1)$$

and

$$\delta_j = \frac{Q_j}{8a}\left(\frac{2-v_w}{G_w} + \frac{2-v_f}{G_f}\right) \qquad (2)$$

where, $R = 1/(R_w + 1/R_p)$-1 is the relative curvature at the contact. R_w and R_p is the local radius of workpiece surface and tip radius of fixture element respectively. Variable E* is composite elastic modulus defined as $1/E^* = (1 – v_w^2) / E_w + (l — v_p^2)/E_p$. Variables v, and G represent the Poisson's ratio, and shear modulus of the material, respectively; the subscripts w and p refer to the workpiece and pin fixture elements, respectively. Variable is the radius of the contact region defined as a = (3PR/4E*). Q_j is friction force calculated by coefficient of friction multiply by pin axial force. Spherical tip deflection is considered by assuming structure of fixture body is rigid.

Linearization of contact stiffness in normal direction for spherical tipped pin fixture element with phenomenon sphere indenting on planar surface is defines as [10]

$$K_z = 13.95\left[\frac{16R_p(E^*)^2}{9}\right]^{1/3} \qquad (3)$$

Length of the pins which is the distance from contact position to the pin host will different due to variation of workpiece geometry. Compliant of the pin have significant contribution for clamping stability. Pin length factor is modeled in addition of pin contact tip. Contact stiffness of pin is modeled as a serial spherical pin combined with a cylindrical beam fixed at one end and sheared at the other.

$$K_{bt} = \frac{E\pi R_p^{\ 2}}{L} \qquad (4)$$

$$K_{pt} = \left[\frac{1}{K_z} + \frac{1}{K_{bt}}\right]^{-1} \qquad (5)$$

L is the distance from pin host to sphere center. For the model evaluated in this research, pin stiffness axial (K_z) and radial (K_{pt}) are determined at the time the model is created and assumed constant for variation of forces and workpiece deformations.

Axial reaction force is calculated from the result of deformation in axial direction:

$$F_{am} = \delta 2_z \ K_n \qquad (6)$$

and tangential force of pin is defined by Coulomb friction law of pin :

$$Q_j = \mu \ F_{am} \qquad (7)$$

5. MODEL FOR FREE FORM GEOMETRY

Free form geometry may be designed using variety of geometrical formulations. A part model may be created using a surface equation such as B-Spline or NURBS or combination between Surface and Features base modeling.

Contact model between pin and workpiece surface is defined by three vectors; one normal vector and two tangential vectors. Normal vector is obtained by interfere operation between pin and workpiece. Vector is determined by the direction from contact point and center of pin. Fig.2 shows CAD simulation to get contact normal vector.

A tangential vector represents the spring model for restrain the workpiece from slip. First vector is defined as the vector parallel to x axis of world coordinate system. Another vector is the cross product of normal and first tangential vectors.

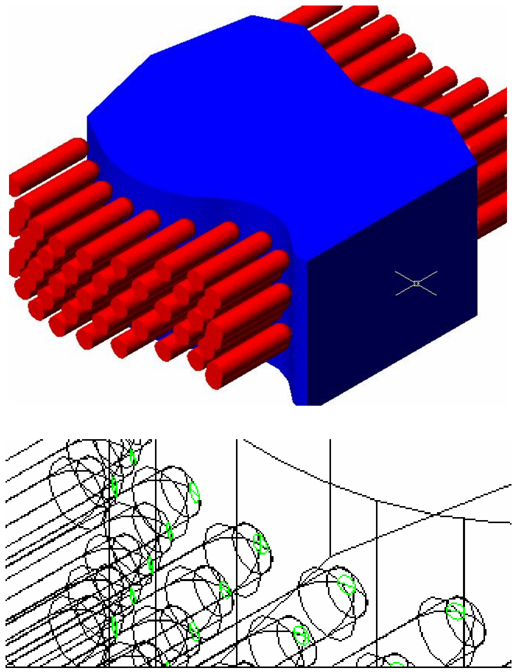

FIGURE 2: Solid Interfere evaluation to obtain Contact and surface normal

6. FINITE ELEMENT MODELING

Finite element analysis using Ansys software is utilized to determine the deformation during clamping. Workpiece model is imported from CATIA V5 CAD software and SOLID95 is selected as material type for meshing. As mentioned in the previous section, three springs are used for a model of a pin and COMBIN14 is selected as spring model. Real constants of the spring will be varying for every pin respect to workpiece geometry. Value of Real constants is pin stiffness for axial and tangential direction. Slip is evaluated by comparing pin radial deflection and workpiece node radial deformation.

Workpiece geometry is modeled using Catia software and imported to Ansys and meshed using VSEL command. For PSO Evaluation, the selected area where the pins are contacted is further refined using "NREFINE" command. Pin is located to the node which is closest to actual pin position. Obtaining the closet not is performed using NODE(PUX(J),PUY(J),PUZ(J)) command. PUX,PUY and PUZ are actual pin coordinate while J is pin index. Following script is codes for refining mesh at pin locations.

```
!left side pins
*DO,J,1,JPIN/2
```

```
    *if,CPU(J),EQ,1,THEN
          NUPIN = NODE(PUX(J),PUY(J),PUZ(J))
          NREFINE,NUPIN, , ,1,1,1,1
    *endif
*ENDDO

!right side pins
*DO,J,1,JPIN/2
    *if,CPL(J),EQ,1,THEN
          NLPIN = NODE(PLX(J),PLY(J),PLZ(J))
          NREFINE,NLPIN, , ,1,1,1,1
    *endif
*ENDDO
```

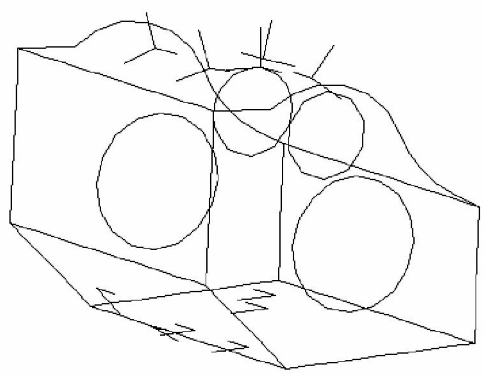

FIGURE 3: Pin-Workpiece Contact model

Fig. 3 shows a spring orientation for clamped workpiece. Support for upper side has three springs while lower side by two vectors. One another vector for lower side is hydraulic clamping with direction always parallel to pin axial axis.

7. HYBRID EVALUATION USING PSO ALGORITHM

Genetic algorithms have no mechanisms for identification absolutely the best solution of particular problem. However, a solution is "better" only in comparison to other, presently known solutions. Algorithm to obtain an optimal solution has to be tested with another way to check whether a solution is optimal. Hybrid technique is second optimization step that runs after the genetic algorithm terminates in order to improve the value of the fitness function. The hybrid function uses the final point from the genetic algorithm as its initial point. A hybrid function can be specified to improve the result.

In order to obtain better clamping position, hybrid evaluation is utilized by combining GAs with PSO algorithm. The PSO algorithm is utilized to determine the best position of the workpiece by shifting around y and z position. Particle Swarm Optimization (PSO) is a population based stochastic optimization technique inspired by social behavior of bird flocking or fish schooling.

PSO is initialized with a group of random particles (solutions) and then searches for optima by updating generations[15]. In every iteration, each particle is updated by following two "best" values.
After finding the two best values, the particle updates its velocity and positions with following equations.

$$v[] = v[] + c1 * rand() * (pbest[] - present[]) + c2 * rand() * (gbest[] - present[]) \tag{7}$$

$$present[] = present[] + v[] \tag{8}$$

v[] is the particle velocity, present[] is the current particle (solution). pbest[] and gbest[] are defined as stated before. rand () is a random number.

There are two variables are used for evaluation using PSO algorithm. Two variables for the pin left and right side was used for GAs and another two variables, that are workpiece position in y and z is utilized for PSO evaluation. Pins configuration for left and right side it has been determined by GA to obtain the best configuration is further evaluated using PSO algorithm to obtain optimum positions of workpiece around the best configurations.

In order to reduce the time of calculation, larger mesh size is selected for GAs evaluation and refined mesh at clamping pin position is performed for PSO. The best position from range between -5.0 to 5.0 in y and z position is searched. Amount of movement is determined by PSO rules. Pins position and contact vectors are recalculated for new location of workpiece. Calculation is performed by sending a message to CAD software using Dynamic Data Exchange (DDE) interface function.

Twenty numbers of iterations and ten population sizes has been used with 0.9 initial inertia weight and 0.4 for final inertia weight.

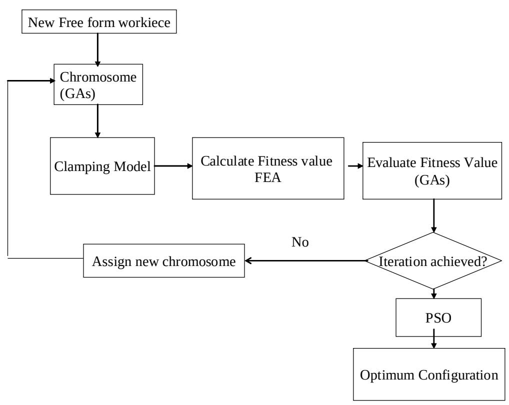

FIGURE 4: Hybrid evaluation scenario

Fig. 4 shows the overall procedure of optimization process with sequence explained as follows. New free form geometry is modeled using a CAD software. Initial configuration is assigned through a random number. Number is then converted to a binary value represent pin configuration. Clamping model for FEA process is generated respect to pin configuration model. Configuration model is evaluated using FEA software to obtain fitness value. Fitness value is then evaluated by GA rule for next generation of configuration with iteration process. Finally PSO is used for fine tuning the result obtained form GAs evaluation.

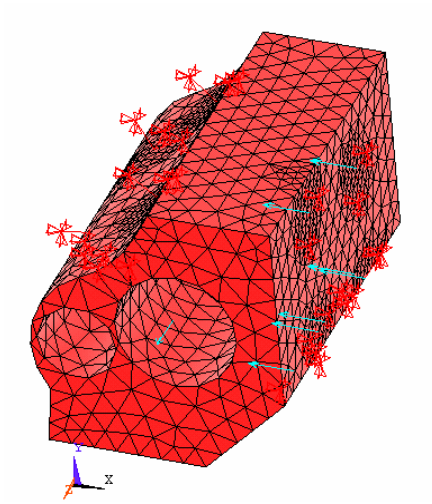

FIGURE 5: Sample workpiece evaluated using FEA for final clamp configuration

8. CASE STUDY

A prismatic 3D part model is used with geometry as shown in Fig. 5 and material properties as listed in Table 2. Cutting force is applied using three forces in x, y and z directions. There are eight pins in each side is applied to the model. Result of FEA computation written using *GET and *VWRITE command is further evaluated using functions created and executed inside Matlab for finding optimum clamping configuration using GAs and PSO. The material properties of the workpiece and pin elements are given in Table 1.

Table 1 Table Material Properties used for FEA

	Workpiece	Pin element
Material	Alloy Steel	Tool Steel
Young's modulus (GPa)	206	217
Shear modulus (GPa)	73	73
Poisson's ratio	0.3	0.3
Static friction coefficient	0.35	

The evaluation source codes are created using Matlab and interfaced with Ansys for calculation the objective function. First process is assigning initial parameters such as number of iteration, population size and generating meshed workpiece model with no supporting and clamping pin. Meshed workpiece is used to obtain the node number for contacted pins. Second process is generating pin workpiece model with configuration as defined by chromosome codes. Spring constant for used pins in radial (Kr) and axial (Ka) are calculated and the result is stored in pin-workpiece model data. The next process is evaluation the clamping model using FEA to obtain maximum deformation and deformation at pin contacted nodes. Deformation data is used to calculate friction slip and fitness value. Slip in pin contacted nodes is occurring when workpiece tangential deformation is more that pin deformation due to friction force. Configuration is categorized as violation if slip in any contacted pin is observed. The evaluation process is repeated until reach the assigned number of populations and generations.

Optimum configuration obtained from GAs evaluation is then evaluated using PSO to obtain minimum workpiece deformation by shifting the workpiece position. PSO will search the optimum position with the configuration obtained by GAs. Workpiece location in x and z direction are dimension parameters adjusted during iteration processes of PSO evaluation. Random number is generated in the range of pin distance in x and z direction.

The magnitude of 500N clamping force is used for every pin. Cutting force is applied at right surface. Parameter uses during GAs evaluation is listed in Table 2.

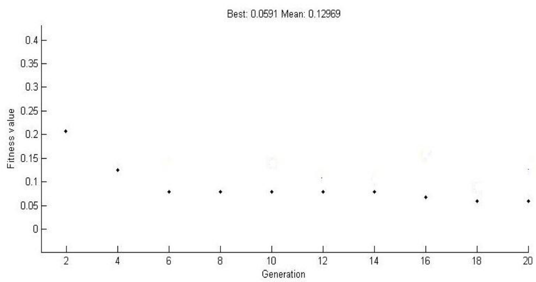

FIGURE 6: Result of Genetic Algorithm for 20 generations

TABLE 2. GAs Parameters

Parameter	Value
Population Size	10
Generations	20
Migration Fraction	0.39796
Crossover Function	1.1316
Mutation Function	0.2907

Result of GAs evaluation with complete iteration is given in Fig. 6. Optimum configuration after 20 generations is 0.0591 with pin configuration chromosome 0000001100101110 and 0000111011001100 for left and right side respectively. Actual pin configuration converting from the chromosome code is shown in the Fig. 5 which have 6 pins for supporting and 7 pins as clamping.

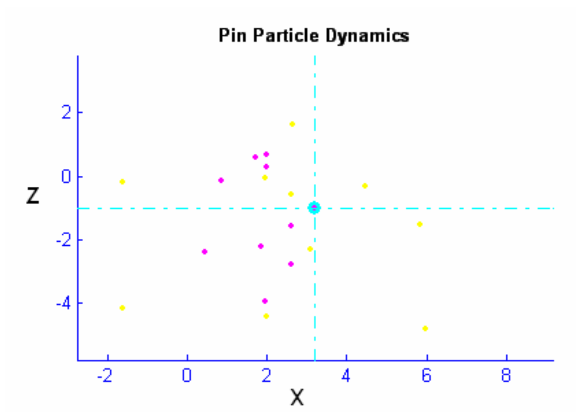

Fig. 7: Dynamics of workpiece Positions during PSO evaluation.

The hybrid function uses the final point from the genetic algorithm as its initial point. A hybrid algorithm is used to improve the result. The second algorithms using PSO are performed to determine the best position of the workpiece. The area between -5.0 to 5.0 in y and z position is searched by dynamically move the workpiece. Value 5.0 mm is the half distance between two closest pins. Process of iteration using PSO rule is shown in Fig. 7. Result after evaluation was shift the workpiece position by 1.3950 and -0.7576 in y and z direction respectively with fitness 0.0541. PSO optimization was moving the workpiece to new location with the less amount of clamping deformation.

9. CONCLUSION

Spherical type pin fixture has been considered as suitable tools to hold a free from workpiece geometry. Evaluation of clamping ability has been performed through Finite Element Analysis for computation of workpiece deformation and detection of slip. Three springs for representing a pin contact vectors possible to reduce the calculation time during iteration process.

Optimization of pin configuration and position for pin type fixture was enabling to minimize workpiece deformation during clamping. The simulation model developed using Genetic Algorithms and PSO algorithms integrated with Finite element method enable to obtain the better configuration of pin respect to minimum deformation.

Optimization technique was performed using hybrid algorithms, GAs and PSO, with four input parameters. Result of optimization process enables to obtain the better pin configurations and clamping positions.

ACKNOWLEDGEMENT

This research is supported by a grand from FRGS 2007 with contract number FRGS 0106-2.

REFERENCES

[1] Afzeri, A.G.E. Sutjipto, A.K..M Nurul Amin, Riza Muhida, 2005, Pin type reconfigurable Clamping ability evaluation for Setup-Free Technology, ICOMMS, Kuala Lumpur.

[2] J.H. Yeh, F.W. Liou, 1999,Contact condition modelling for machining fixture setup processes, Int. J. Mach. Tools Manuf. 39 787- 803.

[3] R.O. Mittal, P.H. Cohen, B.J. Gilmore, 1991, Dynamic modelling of the fixture-workpiece system, Robot. Comput.-Integr. Manuf. 8 (4) 204- 217.

[4] R.J. Menassa, W.R. DeVries, 1991, Optimization methods applied to selecting support positions in fixture design, ASME Journal of Engineering for Industry 113 412- 418.

[5] N. Amaral, J.J. Rencis, Y. Rong, 2004, Development of a finite element analysis tool for fixture design integrity verification and optimisation, International Journal of Advanced Manufacturing Technology 21 411- 419.

[6] E.Y.T. Tan, A.S. Kumar, J.Y.H. Fuh, A.Y.C. Nee, 2004, Modeling, analysis and verification of optimal fixturing design, IEEE Transactions on Automation Science and Engineering 1 (2) 121- 132.

[7] Necmettin, K., 2006, Machining fixture locating and clamping position optimization using genetic algorithms, Computers in Industry 57 112- 120.

[8] A.S. Kumar, V. Subramaniam, K.C. Seow, 1999, Conceptual design of fixtures using genetic algorithms, International Journal of Advanced Manufacturing Technology 15, pp 79- 84.

[9] Y.G. Liao, 2003, A genetic algorithm-based fixture locating positions and clamping schemes optimization, Proceedings of the Institute of Mechanical Engineers. Part B, Journal of Engineering Manufacture 217, pp 1075- 1083.

[10] Shane P. Siebenaler, Shreyes N. Melkote, 2006, Prediction of workpiece deformation in a fixture system using the finite element method, International Journal of Machine Tools & Manufacture 4651- 58.

[11] A.Y.C. Nee, K. Whybrew, A. Senthil Kumar, 1995, Advanced Fixture Design for FMS, Springer, London.

[12] Haiyan Deng, Shreyes N. Melkote, 2006, Determination of minimum clamping forces for dynamically stable fixturing ,International Journal of Machine Tools & Manufacture 46, 847- 857

[13] Anand Raghu, Shreyes N. Melkote, 2004, Analysis of the effects of fixture clamping sequence on part location errors, International Journal of Machine Tools & Manufacture 44 373- 382

[14] Ibrahim M. Deiab, Mohamed A. Elbestawi, 2005, Experimental determination of the friction coefficient on the workpiece-fixture contact surface in work holding applications International Journal of Machine Tools & Manufacture 45 705- 712.

[15] http://www.swarmintelligence.org/tutorials.php

[16] Afzeri, A.G. E. Sutjipto, A.K.M. Nurul Amin, Riza Muhida, 2005, Determination of pin configuration for clamping fixture by means of solid model contact analysis, Proceedings of the International Conference on Mechanical Engineering (ICME), Dhaka, Bangladesh.

NOMENCLATURE

c1 First learning factors of PSO algorithm.
c2 Second learning factors of PSO algorithm.
δ_z spherical clamping static deformation at axial direction
δ_j spherical clamping static deformation at radial direction
$\delta 2_r$ pin static deformation at radial direction
$\delta 2_j$ pin static deformation at tangential direction
E elastic modulus
F_a axial reaction force at *j*th pin
G Shear modulus
v Poisson's ratio
K_z pin stiffness at axial direction
K_{bt} radial stiffness of cantilever bream fixed at one end
K_{pt} spherical pin stiffness for tangential direction
L Pin length, distant from host to contact surface
P clamping force
Q tangential contact forces of pin.
R Pin radius
μ Static friction coefficient

Purpose engineering for Contextual Role-Based Access Control (C-RBAC)

Muhammad Nabeel Tahir m_nabeeltahir@hotmail.com
Multimedia University, Melaka
75450, Malaysia

Abstract

Distributed and ubiquitous computing environments have brought enormous efficiency to the collection, manipulation and distribution of information and services. Although this efficiency has revolutionized countless organizations but it has also increased the threats to individual's privacy because the information stored within the collection of heterogeneous distributed components is sensitive and requires some form of access control. The way to protect privacy in this age of information technology requires such access control system that can accommodate organization requirements to protect privacy of individuals with ease in management and administration of resources. Among those requirements, purpose inference is one of the major problems as the total access control decision mainly relies on the user intentions/purposed. This work in this paper is an attempt to provide purpose engineering semantics that we use for the proposed contextual role-based access control model (C-RBAC) in order to comply with HIPAA.

Key words: Purpose Engineering, Intentions, C-RBAC, Purpose Hierarchy

1 INTRODUCTION

With the development of distributed healthcare systems and pervasive availability of information, prevention of fraud and abuse has become an ever greater issue. The introduction of HIPAA law provides a framework for ensuring the security of medical data especially the electronic versions and maintaining patients' privacy. Care is needed to ensure that every pervasive healthcare system maintains the privacy of personal health information by implementing comprehensive solutions that are both technically sound and legislatively compliant. On the other hand, unauthorized disclosure of health information can have serious consequences including refusal of prospective employment, difficulties in obtaining or continuing insurance contracts and loans, and personal embarrassment [1]. Many studies resulted frameworks, languages, models to preserve privacy of patients. Privacy in [2] has been defined as "The right of an individual to be secure from unauthorized disclosure of information about oneself that is contained in documents".

An access control model based on RBAC to protect privacy in a distributed health care information systems, based on the notion of consent, has been presented in [3]. The authors argued that constraints in RBAC do not provide an elegant solution especially with the role hierarchies. For example if a constraint is applied to the role of a doctor, then its child role (podiatrists) will also inherit the constraints of the role. Therefore it is not easy to execute a policy of the form provide access to all doctors except Dr. X. In their work, a patient's access policy have been recorded and enforced through a consumer centric role called care-team role (CTR) that consists of four main components: list of roles that has been allowed to access patient's health information, list of roles that have been denied to access to patient's health information, the access privileges, and administrative information about the CTR such as its ID and description. A similar approach has been proposed [4]. However, their work does not provide any mechanism to ensure the mapping of patient formalized policies and consents into CTR. Overall there has been no concrete framework of RBAC with privacy-based extensions. An extended framework of RBAC with privacy based extensions to control information access in e-Health has been presented [5]. Authors proposed an aggregation decision-making layer interacted with a set of autonomous RBAC models to aggregate PHI in e-Health care informatics. Although semantic definitions of role authorization with purposes, recipients, retentions and obligations as sets of privacy-based entities has been provided, their work has not shown how these privacy-based entities can be engineered and enforced into e-Health framework. The work also has not provided any purpose driven approach, purpose hierarchies and relationships between subject roles and purposes (spatial purpose role).

The info space concept as the trust boundary and the privacy tag for privacy control in ubiquitous systems has been presented in [6]. Jiang & Landay [7] discussed how the user can be notified about data collection by sensors and how a policy can be negotiated. However these two privacy frameworks referred to a general ubiquitous computing or context-aware computing environment and have not been directly applicable to healthcare information systems. More relevantly, the work [8] analyzed the dependability issues in U-Healthcare. Beckwith [9] discussed the perception of privacy based on the case study of a sensor-rich, eldercare facility. The work in [10] presents a method to control access to any sensor data recorded by a personal ubiquitous healthcare system. Their approach has been based on the concept of mediator that logically sits between a personal healthcare system used by the patient and any clinical system used by the caregiver. However, their proposed architecture does not cope with such dynamic requirements of ubiquitous environment. On the other hand, many information privacy and security laws tailored their protections according to the purpose of the use or disclosure, rather than basing that solely to the particular characteristics of the data itself. Purposes present user's intentions for which he/she requests access to use resources. Few definitions of purposes have been described in the literature. For example, purpose "an anticipated outcome that is intended or that guides your planned actions" [11]. Purpose in [12] has been described as the reason for which organizations' resources are used. P3P [13] defined the purpose as "the reason for data collection and use" and specify a set of purposes including current, admin, contact, telemarketing etc.

2 Purpose Context

There are several ways to capture purposes/intentions of the user who request to access resources. First possible method is to register each application with an access purpose. As applications have limited capabilities and can perform only specific tasks, it should be ensured that data users use them to carry out only certain actions depending on the associated access purposes. This method, however, cannot be used in distributed and ubiquitous environment for applications as it may access various data and resources for multiple purposes. Another possibility is to state access purpose(s) along with the requests to access organization resources and confidential data. Although this method is simple and can be easily implemented however, the overall privacy that the system is able to provide relies entirely on the users' trustworthiness as it requires complete trust on the users. Lastly, the access purposes can be dynamically determined by the system based on the current context. For example, consider the case where the user with the role DayDutyDoctor sends a request to access a patient record. From this context (i.e., the job function, role, the nature of the data to be accessed, the application identification, time of the request, location of doctor), the system can reasonably infer that the purpose of the data access must be "routine checkup". The advantage of this approach is that many access purposes can be defined for the same values of context information in order to provide a flexible way of making access control decisions. However the key challenge for implementing this method is to engineer context information accurately and efficiently. This work has defined purpose for C-RBAC model as:

Definition 1 ***(Purpose)*****:** Purpose is the intention of the user that is computed based on the contextual values of the user's current environment through which the user is requesting access to use resources.

$$Purpose\ p \rightarrow SPR \times T \times LOC\_ATR$$

where SPR $\in$ Spatial purpose roles, T is time interval borrowed from Joshi, Bertino, Latif, & Ghafoor [14, 15] and LOC_ATR is a set of attributes e.g. user motion direction, motion speed, user location and distance from resource such that given the user session s, SLOC_ATR (s:SESSION) represents the current contextual values for the session s activated by the user u.

$$LOC\_ATR: \bigcup_{s \in SESSION} SLOC\_ATR(s)$$

The number of contextual variables and its values may vary based on the organizations' requirements. For example, some organizations may consider time t, and role r, of the user u to compute the purpose of the user. For example, if user u (Bob) with the role r (doctor) sends a request to access a patient record pr of patient between 7am to 7pm, then the purpose p is RoutineCheckup. Similarly, some organizations may consider time t, location l and role r of the user u to compute the purpose of the user. For example, if user u (Bob) with the role r (doctor) sends a request to access a patient record pr of patient from general ward where patient is admitted then the purpose p is RoutineCheckup. In order to elaborate further, consider the scenario in Figure 1 where there are four departments in a hospital: ICU Ward, General Ward, Laboratory and X-Ray Department. Assume that Bob, a cardiologist doctor is assigned to ICU ward. He is also attached to Laboratory as the Laboratory Head. When Bob login into the system, the system will automatically enable the roles that are assigned to Bob depending on his location. In this scenario, Bob will get all the roles that are assigned to him at the location of ICU Ward. Assume that for some reason, either for a normal routine checkup or for emergency calls, he has to go to the General Ward. When Bob walks to the General Ward, he will pass two other departments, i.e. Laboratory and X-Ray Department. The system can easily get the physical position of Bob through GPS (external), access points or sensors (internal) and computes the logical location of Bob. If the relative location overlaps between two regions for example the doctor's logical location overlaps with the Laboratory and X-Ray Department, then all the roles that are assigned to Bob will be enabled automatically although Bob is on his way to General Ward. However, if the system is capable of monitoring the user movement direction then it can easily infer that Bob's intention is to go to the General Ward rather than Laboratory or X-Ray Department.

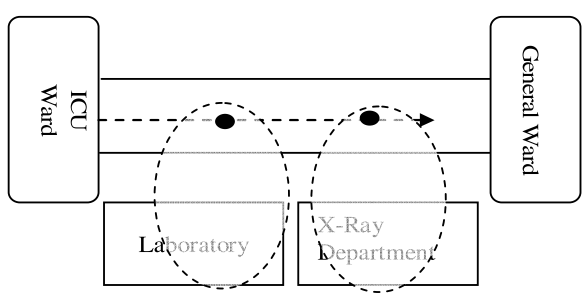

Figure 1: Relative Location Overlapping.

2.1 PURPOSE HIERARCHY

Like subject roles, purposes also have a hierarchical relationship among them. For instance, the purposes MinorOperations and MajorOperations can be grouped together by a more general purpose Operation. This suggests that purposes can be organized in hierarchical relationships to simplify the management of the purposes. The hierarchical relationship among different purposes is shown in figure 2 where each node represents the purpose and each edge represents the parent/child relationship. The next definition formalizes the above discussion.

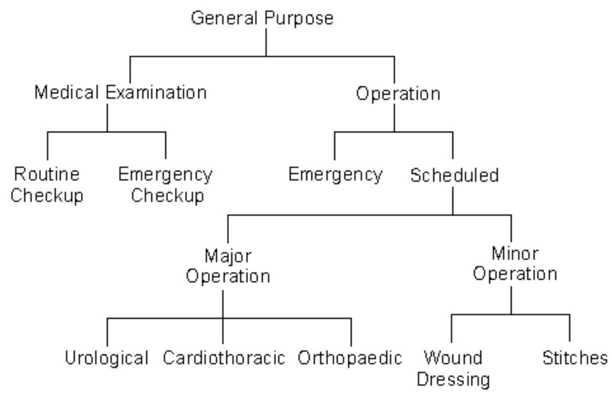

Figure 2: Purpose Hierarchy in C-RBAC.

Definition 2 ***(Purpose Hierarchy)***: Let P be a set of purposes defined within the system. A hierarchical relationship is defined with ≤ between purposes such that pi ≤ pj means that pj is child of pi or pi is a parent of pj.
Figure 2 shows an example of hierarchical relationship between purposes. MajorOperation ≤ Cardiothoracic means that purpose MajorOperation is a parent purpose of Cardiothoracic. In another words, the subject role or location assigned to the purpose MajorOperation will also be assigned automatically to Cardiothoracic.

Another novelty in this work has been the definition of relation between purposes and locations. A notion of spatial purpose (SP) is introduced that is defined as a purpose in relation with location. It must be noted that multiple spatial purposes can be defined at one particular location, LHS and LHI level.

Definition 3 ***(Spatial Purpose)***: Spatial purpose is a purpose defined over a particular location such that;

Spatial Purpose SP <sp, lloc, p>

where sp is spatial purpose name such that sp ∈ P (universal set of all spatial purposes defined in a system) and lloc is a logical location such that lloc ∈ LLOC, defining the boundaries for sp and p is a purpose such that p ∈ P.

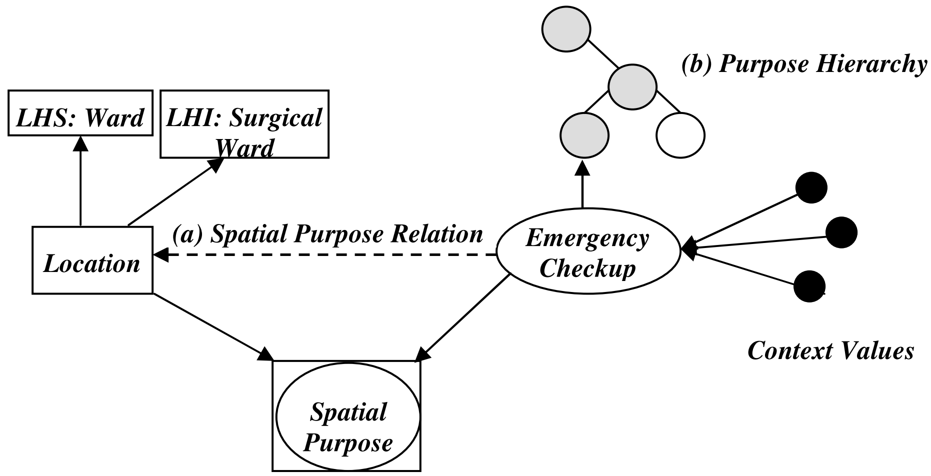

Figure 3: Spatial Purpose (*SP*) Relationship.

Figure 2 shows (a) hierarchical relation between purposes as defined in figure 3 and (b) spatial purpose relation in which purpose *EmergencyCheckup* is defined over logical or physical location.

2.2. SPATIAL PURPOSE WITH LHS AND LHI

In common business environments it is also possible to define spatial purposes for a group of hierarchically organized locations. The proposed spatial purpose engineering is flexible enough to allow security administrator to define spatial purposes for LHS in order to allow a group of users to perform common departmental activities with generalized purposes. For example if the hospital policy states that all medical staff in wards can check the availability of medical doctors in all wards for the purpose of emergency checkup then a spatial purpose can be defined at LHS:Ward level to allow all medical staff in wards to acquire EmergencyCheckup purpose. The advantage of this approach is that spatial purposes can be defined only once and assigned to LHS that propagates spatial purpose to all nodes of hierarchically organized logical locations. This reduces the overhead of defining the same spatial purposes for different logical locations. It also eases the management of spatial purposes especially in large organizations where a same purpose is required at many different locations. As LHS can have many instances (LHI) [16]; each defined with a unique name. This means that spatial purposes defined at LHS level will also be assigned to all instances (LHI) instantiated through LHS. Additionally, spatial purposes can also be defined at LHI level. This is a case where organizations want to allow users from some specific locations to acquire purposes to perform activities. For example if the hospital management wants to allow only those staff members who are on duty in surgical ward to check the availability of medical doctors for emergency checkup then spatial purpose EmergencyCheckup will be defined at LHI:SurgicalWard level only to allow staff in surgical ward only to acquire EmergencyCheckup purpose.

Figure 3 shows spatial purposes defined at LHS:Ward and LHI:SurgicalWard level along with a set of purposes (through hierarchical relationship) {MajorOperation, Scheduled, Operation and GeneralPurpose} for all wards as <EmergencyCheckup, Ward> at LHS level and for surgical ward only as <EmergencyCheckup, SurgicalWard> at LHI level.

Definition 4 ***(Spatial Purpose with LHS)*****:** Let lhs is location hierarchy schema and p is a purpose such that $p \in P$ and $lhs \in LHS$, spatial purpose with LHS is defined as:

Spatial Purpose SPlhs <splhs, p, lhs>

where splhs is a spatial purpose name, p is a purpose defined at lhs. SPLS is defined as a spatial purpose logical location set, a set of logical locations defining the boundaries of splhs such that LhsOccurencelloc(lhs) → SPLS = {lloc1, lloc2…llocn}, where lloc ∈ LLOC.

Definition 5 ***(Spatial Purpose with LHI)*:** Let lhi is location hierarchy schema and p is a purpose such that p ∈ P and lhi ∈ LHI, spatial purpose with LHI is defined as:

Spatial Purpose SPlhi <splhi, p, lhi>

where splhi is a spatial purpose name, p is a purpose defined at lhi. SPPS is defined as a spatial purpose physical location set, a set of physical locations defining the boundaries of splhi such that LhiOccurenceploc(lhi) → SPPS = {ploc1, ploc2…plocn}, where ploc ∈ PLOC.

Spatial Purpose with SDOM:

As explained in [17], domains may have multi-domain and multilevel-domain relationships among them as spatial domains are defined over LHS and LHI. Another novelty in this work is the definition of two types of relationships between purposes and spatial domains Internal Spatial Purpose relationship (INT_SPSDOM) and External Spatial Purpose relationship EXT_SPSDOM. A relationship INT_SPSDOM exists when a purpose p defined at SDOM level to be inherited to all schemas or instances within spatial domain. These relationships are represented as:

Definition 6 (Spatial Purpose with Spatial Domain): Let SDOM is spatial domain and p is purpose such that p ∈ P, we define INT_SPSDOM as:

(a) Spatial Purpose INT_SPSDOM <spSDOM, SDOM, p>

It is mentioned earlier that spatial domains are defined over LHS and LHI. In case of SDOM over LHS, SS is defined as schema set that contains location hierarchy schemas covered within SDOM such that SS → SchemaDomain(SDOM) = { lhs1, lhs2,… lhsn }, where lhs ∈ LHS and PSET as purpose set that contains purposes defined at spatial domain level such that PSET → GetParentPurposes(p) = { p1, p2,… pn }. Similarly IS as a set of location hierarchy instance covered within SDOM through LHI such that IS → InstanceDomain(SDOM) = { lhi1, lhi2,… lhin }, where lhi ∈ LHI.

EXT_SPSDOM relationship defines spatial purposes at domain level so that whenever a user from one domain such as SDOM1 sends request to access resource of another domain SDOM2, SDOM2 grants/denies access to resource based on the type of user request and the EXT_SPSDOM spatial purpose relationship defined with SDOM1. For example, a research domain may establish Research purpose relationship with laboratory domain in order to access PHI for the purpose of research. Similarly an insurance company may access patient insurance information from hospital for the purpose of InsuranceClaim as shown in figure 4.

(b) *Spatial Purpose* EXT_SP_{SDOM} $<SDOM_i, SDOM_j, p>$

where p is a purpose describing that SDOMi can access the resources of SDOMj for the purpose(s) defined in PSET.

Figure 4 shows that purposes defined through INT_SPSDOM relation over surgical and emergency domain are inherited at all respective locations (physical and logical locations through lhs and lhi) based on their inclusion within spatial domain whereas purpose defined through the relation EXT_SPSDOM between emergency ward and laboratory shows that emergency ward domain can access test results in laboratory for the purpose EmergencyCheckup.

By definition [17] (a), relationship can be defined as INT_SPSDOM <Emergency, EmergencySDOM, EmergencyPurpose> means that access request for the purpose of EmergencyCheckup can be made from all locations defined within the domain EmergencySDOM in order to access its resources. The logical location set SS in this case will be generated as SS = {Ward, Ward} and it will further propagate purposes to all logical/physical locations covered by Emergency domain such that { PatientFloor, StaffFloor, Reception, EmergencyRoom, TempObrArea, NurseOffice, DoctorOffice}. Similarly by definition of spatial purpose over domains [17] (b), EXT_SPSDOM relationship between two spatial domains can be defined as <EmergencySDOM, LaboratorySDOM, EmergencyCheckup> which means that request from EmergencySDOM to LaboratorySDOM can only be granted for the purpose EmergencyCheckup.

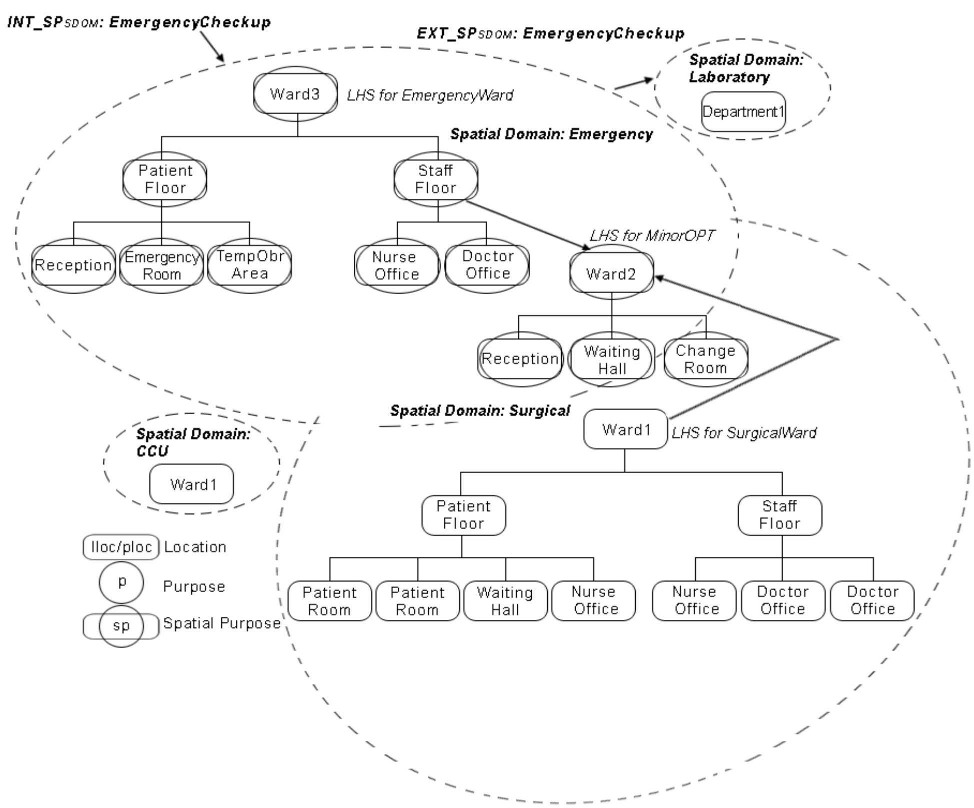

Figure 4: Spatial Purpose Relationships Defined Over Spatial Domain.

2.3 PURPOSE MODULE AND SPECIFICATION TOOL

Figure 5 shows GUI for purpose specification tool and figure 6 shows the architectural representation of purpose module. Context Collector collects contextual values from the underlying technology. Context Generator then assigns these collected values to context attributes defined for C-RBAC model based on which Purpose Inferor deduces the purpose of the user. Purpose Manager (PM) manages all purposes within the system including addition or edition of purposes. Purpose Activator (PA) activates/deactivates purposes based on the constraints defined for context values. Based on the purposes defined through PM, Purpose Hierarchy Manager (PHM) defines and manages hierarchical relationships among purposes. SP Manager manages the Spatial Purpose (SP) relationship defined between location and purpose.

SP-LHS Allocator defines SP between LHS and purpose whereas and SP-LHI Allocator defines SP between LHI and purpose. As all purposes defined for LHS will be propagated at LHI level. This propagation of purposes from LHS to LHI is done by SP Propagator. Lastly, SP-SDOM Relationship Manager manages relationship between SDOM and purposes based on the spatial relationships (INT_SPSDOM, EXT_SPSDOM).

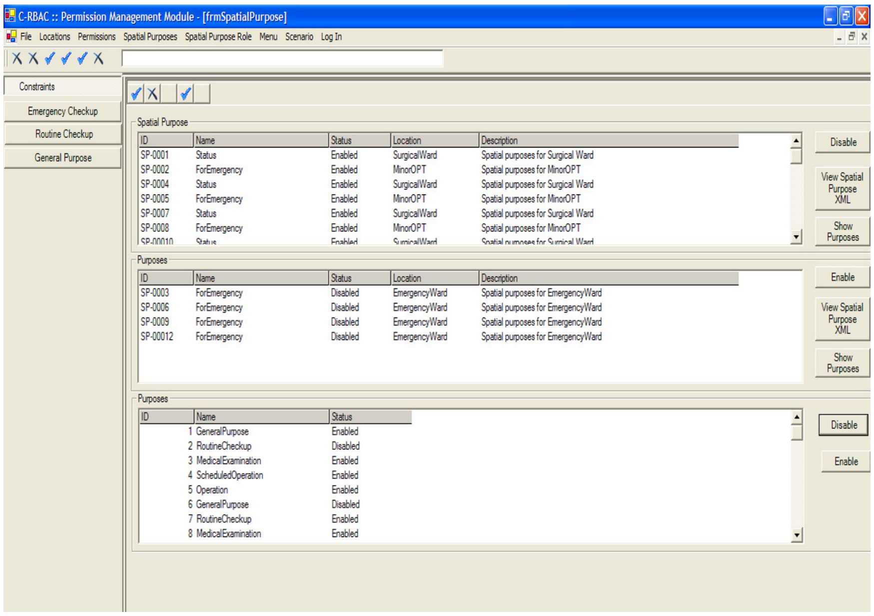

Figure 5: GUI of Purpose Module for C-RBAC.

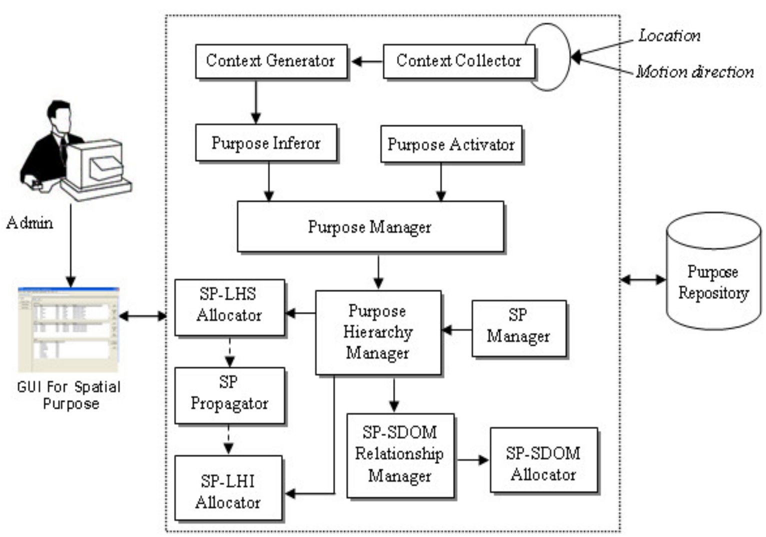

Table 1: Purpose and Spatial Purpose Functions.

Table 1 shows purpose and spatial purpose functions used by purpose module. These functions are used to add a new purpose, to infer the purpose based on the context values, to check the state of the purpose that whether the given purpose is parent or child, to retrieve parent/child purposes, to retrieve purposes defined at different spatial granularities.

3 CONCLUSION

In this paper, purpose model for contextual role-based access control model has been presented for privacy access decisions. Purpose semantics and some definitions including purpose, purpose hierarchy, purpose relation with location model (spatial purpose) have been presented that will be used by C-RBAC model in order to make privacy aware access control decisions. In order to support our idea of purpose engineering, the paper then presented a system implementing the proposed purpose engineering semantics. Lastly, purpose and spatial purpose functions are presented that are used by our prototype.

4. REFERENCES

[1] Rindfleisch, T. (1997). Privacy, information technology, and health care. Communications of the ACM, 40(8), 93–100.

[2] Archives & Records Management Handbook. (2003). Retrieved January 2, 2008, from http://osulibrary.oregonstate.edu/archives/handbook/definitions/.

[3] Reid, J., Cheong, I., Henricksen, M. & Smith, J. (2003). A Novel Use of RBAC to Protect Privacy in Distributed Health Care Information Systems. Paper presented to Information Security and Privacy, 8th Australasian Conference, ACISP, Wollongong, Australia.

[4] Bacon, J., Lloyd, M. and Moody, K. (2001). Translating role-based access control policy within context. In Workshop on Policies for Distributed Systems and Networks, Springer-Verlag, 107–120.

[5] Patrick, C., Hung, K. and Zheng, Y. (2007). Privacy Access Control Model for Aggregated e-Health Services. Proceedings of the 2007 Eleventh International IEEE EDOC Conference Workshop, Maryland U.S.A, 12-19.

[6] Langheinrich, M. (2001). Privacy by Design — Principles of Privacy-Aware Ubiquitous Systems. In “Ubicomp 2001”. Retrieved January 22, 2008, from http://www.vs.inf.ethz.ch/publ/papers/privacy-principles.pdf.

[7] Jiang, X. and Landay, J. A. (2002). Modeling privacy control in context-aware systems. IEEE Pervasive Computing, 1(3), 59-63.

[8] Bohn, J., Gartner, F. and Vogt, H. (2004). Dependability Issues of Pervasive Computing in a Healthcare Environment. *Security in Pervasive Computing, First International Conference, Boppard, Germany*, 53-70.

[9] Beckwith, R. (2003). Designing for Ubiquity: The Perception of Privacy. IEEE Pervasive Computing, 2(2), 40–46.

[10] Beresford, R. and Stajano, F. (2004). Mix zones: User privacy in location-aware services. Proceedings of the 2nd IEEE Annual Conference on Pervasive Computing and Communications Workshops (PERCOMW04), Orlando, Florida, pp. 127.

[11] Definition of the purpose on the Web. Retrieved July 30, 2007, from: http://www.google.com/search?hl=en&rlz=1T4GFRC_en___MY202&defl=en&q=define:purpose&sa=X&oi=glossary_definition&ct=title.

[12] Byun, J. W., Bertino, E. and Li, N. (2004). Purpose Based Access Control for Privacy Protection in Relational Database Systems. Technical Report 2004-52, Purdue University, USA.

[13] World Wide Web Consortium (W3C). Platform for Privacy Preferences (P3P) Retrieved October 10, 2008, from http://www.w3.org/P3P.

[14] Joshi, J.B.D., Bertino, E. and Ghafoor, A. (2002). Temporal Hierarchies and Inheritance Semantics for GTRBAC. Proceedings of the seventh ACM symposium on Access control models and technologies, Monterey, California, USA, 74-83.

[15] Joshi, J. B. D., Bertino, E., Latif, U. and Ghafoor, A. (2005). A Generalized Temporal Role-Based Access Control Model. IEEE Transactions on Knowledge and Data Engineering, 17(1), 4–23.

[16] Tahir, M. N. (2008). Hierarchies in Contextual Role- Based Access Control Model (C-RBAC). International Journal of Computer Science and Security (IJCSS), 2(4), 28-42.

[17] Tahir, M. N. (2007). Location Modeling for C-RBAC: Contextual Role-Based Access Control Model. International Conference on Information Technology in Asia (CITA), 265-269.

COMPUTER SCIENCE JOURNALS SDN BHD
M-3-19, PLAZA DAMAS
SRI HARTAMAS
50480, KUALA LUMPUR
MALAYSIA